ELSEVIER

Marine Geology 230 (2006) 29–51

MARINE GEOLOGY
INTERNATIONAL JOURNAL OF MARINE GEOLOGY, GEOCHEMISTRY AND GEOPHYSICS

www.elsevier.com/locate/margeo

Anthropogenic markers in the Holocene stratigraphic sequence of the Gulf of Trieste (northern Adriatic Sea)

Stefano Covelli [a,*], Giorgio Fontolan [a], Jadran Faganeli [b], Nives Ogrinc [c]

[a] *Department of Geological, Environmental and Marine Sciences, University of Trieste, Via E. Weiss 2, 34127 Trieste, Italy*
[b] *Marine Biological Station, National Institute of Biology, Fornace 41, 6330 Piran, Slovenia*
[c] *Department of Environmental Sciences, Jozef Stefan Institute, Jamova 39, 6100 Ljubljana, Slovenia*

Received 19 October 2005; received in revised form 18 March 2006; accepted 28 March 2006

Abstract

The Gulf of Trieste is a shallow semi-enclosed marine basin in the northernmost part of the Adriatic Sea that has been affected by the relative rise in sea-level during the Holocene. The sedimentary sequences in three cores, ranging in length from 130 to 320 cm, were investigated through the variability in grain-size parameters, major (Al, Fe, S, N, Ca and Mg) and trace (Ti, Mn, Cr, Ni, Cu, Zn and Hg) elements, organic and inorganic C, $\delta^{13}C$ and ^{14}C dating in order to obtain information on paleoenvironmental evolution and the historical development of heavy metal contamination. The potential sources of pollution are: urban sewage from nearly 400,000 inhabitants, industrial effluents, and 500 yr of Hg mining activity in the Idrija region (western Slovenia), located in the upper basin of the Isonzo river, the main freshwater input to the coastal zone. The conventional ^{14}C ages of bulk sedimentary OC in the basal part of the three cores were 9030±70 (GT1), 8270±50 (GT2) and 9160±120 (GT3) yr BP. An upward increase in highly negative $\delta^{13}C_{org}$ values from the core bottoms indicates that lacustrine-swamp conditions in the study area were rapidly followed by a typical marine depositional environment. Cluster analysis performed on the geochemical data for all subsamples of the three cores identifies several groups with a clear stratigraphic meaning. Factor analysis of the data shows related element groups that can be interpreted as being related to, for instance, the natural contribution from aluminosilicates and carbonates, from organic matter (peat) and the more recent anthropogenic "impact". Predicted natural linear relationships for metal-Al were obtained from the core subsamples and they can be used as a baseline to evaluate metal enrichments on a regional scale. Results show that more recent sediments in the central sector of the Gulf of Trieste are slightly enriched in Cu (max Enrichment Factor EF=2.1) and Zn (max EF=1.6), and noticeably contaminated by Hg (up to 23.32 $\mu g\ g^{-1}$) to a maximum depth of 90 cm and up to 60 times above the estimated regional background (0.13 $\mu g\ g^{-1}$). The Hg historical trend is well correlated with extraction activity at the Idrija mine, thus allowing indicative sedimentation rate estimation and tentative assessment of the rate of Hg accumulation in bottom sediments (from 1.77 to 31.49 mg $m^{-2}\ yr^{-1}$ at the surface). The large inventory of Hg in the core GT2 appeared to be the result of proximity to the fluvial source, which is still active in supplying Hg to the coastal areas and makes the Gulf of Trieste one of the most Hg contaminated area in the whole Mediterranean basin.

Keywords: marine sediments; marine geochemistry; metals; mercury; Holocene; Adriatic Sea

* Corresponding author. Tel.: +39 40 5582031; fax: +39 40 5582048.
E-mail address: covelli@univ.trieste.it (S. Covelli).

0025-3227/$ - see front matter © 2006 Elsevier B.V. All rights reserved.
doi:10.1016/j.margeo.2006.03.013

1. Introduction

Human activity has enhanced the delivery and cycling of heavy metals to coastal zones. Many of these contaminants are toxic to aquatic biota and could have an important impact on the whole ecosystem. Hence, it is important to track the influence of anthropogenic activities on the concentration levels of these contaminants and to understand the processes affecting their changes. Interpretation of human influences requires knowledge in natural baseline concentrations. Most contaminants are associated with the surface of particles and are preferentially transported, accumulated and buried within fine-grained sediments. Cores carefully dated through sedimentary deposits can provide chronologies of contaminant concentrations and input in areas of net sediment accumulation. In the coastal zone, the core chronologies are mostly restricted to sediments in anoxic and abiotic environments where resuspension and bioturbation are minimal (Huh, 1996; Hornberger et al., 1999). In bioturbated sediments such studies are less common.

In this study, variations in sedimentological and geochemical features in radiocarbon dated Holocene stratigraphic sequences from the northern and central part of the Gulf of Trieste, which is affected by several potential pollution sources, were investigated. These variations were placed in a paleoenvironmental context and correlated with results obtained in the southern littoral zone of the gulf (Ogorelec et al., 1981, 1984, 1987, 1997; Faganeli et al., 1991).

Special attention was given to providing pre-industrial background levels of heavy metals for the Gulf of Trieste, particularly for mercury (Hg) because of the long-term mining activity in the Idrija region located in the upper Isonzo river drainage basin, the main freshwater input (Faganeli et al., 1991; Gosar et al., 1997; Covelli et al., 1999, 2001). Sedimentary records of this geochemical tracer were compared with the records of 500 yr of ore extraction in order to reconstruct the Hg depositional history, determine the accumulation rate and calculate the cumulative metal inventory.

2. Environmental setting

The Gulf of Trieste, covering an area of about 500 km^2 in the northernmost part of the Adriatic Sea, is an epicontinental semi-enclosed shelf basin characterised by a very low bathymetric gradient in the northern and central part (40 m/100 km). The main water and sediment supplies to the gulf of Trieste are related to the Isonzo river. Its drainage basin covers about 3400 km^2, extending into both Italy and Slovenia. The average annual flow rate at the river mouth is estimated to be 196.8 $m^3\ s^{-1}$, ranging monthly from 43.1 to 665.9 $m^3\ s^{-1}$ (Interreg II, 2001). The rate of flow can exceed 2500 $m^3\ s^{-1}$ during the autumn floods (RAFVG, 1986). The mean annual solid discharge is 150 g m^{-3}, with peaks of 1000 g m^{-3} during extreme events (Mosetti, 1983).

Sediments vary from medium to fine sands along beaches and the delta front to prodelta muds in mid-Gulf (Brambati et al., 1983). Mesozoic limestone and Eocene flysch are the two prevalent lithologies cropping out in the catchment area. The former prevails in the northernmost alpine chains, the latter outcrops in the hilly and pre-alpine areas bordering the alluvial plain (Stefanini, 1976). Carbonate sediments dominate the marine area near the river mouth. Only the southeasternmost sector of the Gulf, affected by low terrigenous inputs from secondary streams (the Rosandra, the Rizana, and the Dragonja rivers), shows significant amounts of quartzo-feldspathic material (Brambati, 1970), while the carbonate component decreases seawards according to grain-size reduction (Ogorelec et al., 1991).

The Gulf of Trieste is affected by many potential sources of organic and inorganic pollutants, discharged not only by rivers but also by sewers, industrial developments, and activities related to the oil-pipeline terminal in the Trieste harbour area (Olivotti et al., 1986; Adami et al., 1996, 1998).

3. Materials and methods

3.1. Samples collection and analytical procedures

Three sediment cores (10 cm diameter) at sites GT1 (245 cm length; 23 m depth), GT2 (320 cm length; 15 m depth) and GT3 (130 cm length; 25 m depth) (Fig. 1) were collected in 1996 and 1997 from R/V OGS Explora with a gravity corer, sealed on board and stored at +4 °C in a cold room prior to subsampling.

After splitting, the cores were photographed and described macroscopically for lithology and colour variability (Munsell Soil Color Charts, 1975) and for sedimentary structures along with macrofossil content. A half core was examined by X-ray photography to identify faint structures and slight changes in density, texture and mineralogical composition.

Subsampling for water content, grain-size and geochemical analysis was performed by cutting 1-cm-thick slices. Analyses were performed in every 1 cm of the first 25 cm of the cores, every 2 cm (25–50 cm

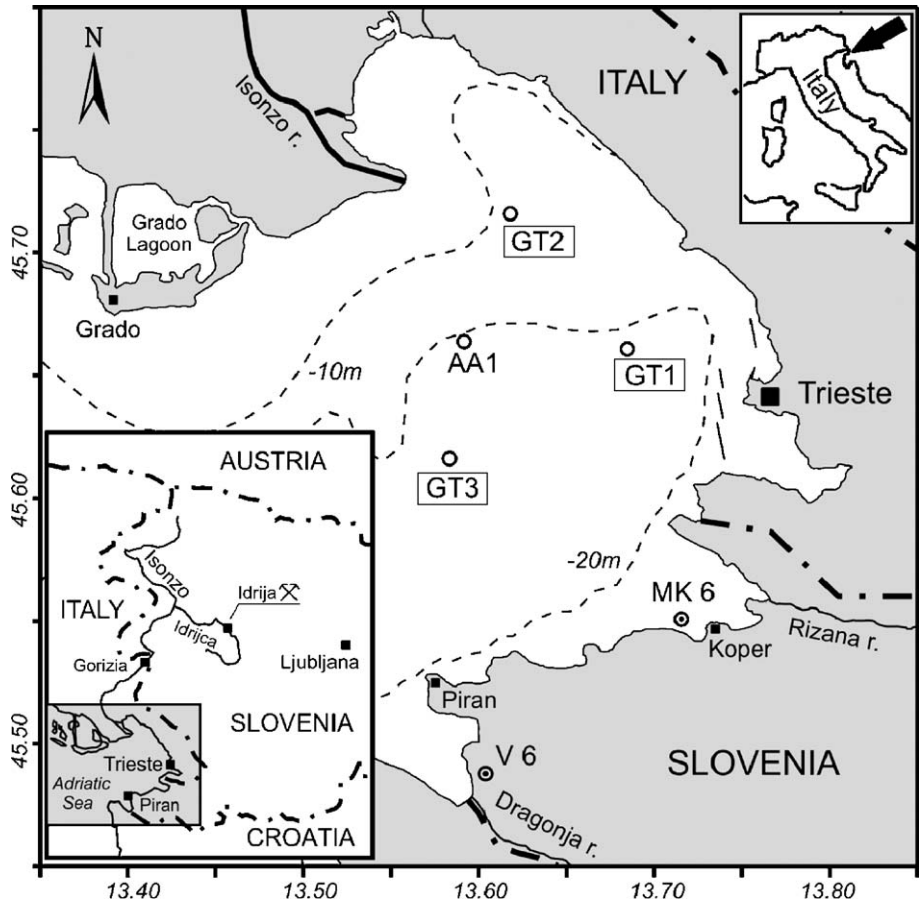

Fig. 1. Index map of the study area with the locations of the sediment cores and the boreholes mentioned in the text.

depth), every 10 cm (50–100 cm depth) and every 20 cm for depths greater than 100 cm.

For grain-size analysis, sediments were wet-sieved through a 53-μm sieve after 48 h of H_2O_2 treatment to remove organic matter. The fraction <53 μm was collected, filtered through 50 Whatman filters and dried at 40 °C. The grain-size distribution of the fine fraction was determined on the basis of the suspension of sediment in distilled water, to which a 0.5 g dm^{-3} Na-hexametaphosphate antiflocculant solution was added, using a Micromeritics Sedigraph 5000 ET Particle Size Analyzer. The water content was calculated on 2–3 g subsamples as loss of weight after oven drying at 105 °C for 24 h.

Major (Al, Fe, Ca and Mg), minor (Ti and Mn) and trace element (Ni, Cr, Cu, Zn) determinations were performed on freeze-dried sediment subsamples. Pebbles, shells and organic debris were removed and the sediment was ground to pass through a 200-mesh (75 μm) sieve. The total decomposition method recommended by Loring and Rantala (1992), using HF + aqua regia in teflon bombs before AAS analysis, was applied for the analytical determination of metals. Hg was determined following the procedure of CV AAS. After overnight decomposition with suprapur HNO_3 in PTFE vessels at 120 °C, $SnCl_2$ and hydroxylamine sulfate were added directly to the vessels and Hg vapours were flushed by air into the measuring cell of a Varian AAS. Totals for C, N and S in the sediments were determined from freeze-dried and homogenised samples, and organic C (OC) after acidification with 1 M HCl, using a Carlo Erba model EA 1108 C–H–N–S elemental analyser at a combustion temperature of 1020 °C (Hedges and Stern, 1984). The precision of the analytical methods, estimated using replicate analyses, is as follows: 5% for C, OC, N and S; 1% for Fe, Al, Ca and Mg; 2% for Mn and Ti; 4% for Ni, Cr and Zn; and 3% for Hg and Cu. The isotopic composition of sedimentary OC was determined after removing carbonates with 1 M HCl. Determination of $\delta^{13}C$ of the OC fraction was carried out after the combustion of samples at 1800 °C using an Europa 20–20 continuous-flow

stable isotope analyser with an ANCA-SL preparation module. The results were expressed in the usual δ-notation in parts per mil (‰). The V-PDB carbonate standard was used for carbon and the analytical precision was ±0.2‰.

3.2. Dating of sediment cores

Bulk sedimentary organic C samples from selected depths in cores GT1 and GT3 were dated, using the standard AMS method of radiocarbon analysis (^{14}C), at the NOSAMS facility (Woods Hole Oceanographic Institution, MA, USA). Radiocarbon dating of GT2 core bulk sediment samples, along with two shell samples from the GT1 and GT3 cores, was performed using AMS by Beta Analytic Inc. (Miami, FL, USA). After acidification the samples were combusted to CO_2, which was then converted to graphite and analyzed along with Oxalic Acid I and II standards (plus process blanks). The counting error in the reported ^{14}C contents averaged ±2% of the measured "age".

3.3. Statistical analyses

For the statistical analyses, calculation of the Pearson's correlation matrix of the variables was firstly performed. *R-mode* factor analysis was then used in the multivariate dataset to extract the principal components on the basis of the factor loadings. The cluster analysis technique (*Q-mode*) was finally applied to the original dataset in order to classify sediment samples in homogenous groups based on their similarity.

4. Results

4.1. Stratigraphy and sediment dating

The sedimentary sequences in the three cores are depicted in Fig. 2. The upper section of the core GT1 (0–155 cm) is composed of olive grey silty clay, well hydrated at the top (47.7% average water content) and changing into a more compact grey sediment of similar texture with downcore depth. Macrofauna is represented by scarce fragments of bivalves and gastropods (*Turritella* sp.) at the top, though they are more abundant near the lower limit, which is marked by a sharp horizontal colour change. Two distinct layers rich in *Ostrea edulis* were found at 78–82 and 113–123 cm depth. The following section (155–225 cm) is characterised by dark grey silty clay with a mottled aspect due to greenish brown lenses of clay. Peaty lenses are irregularly dispersed between 172 cm and the lower limit of this unit where shelly fragments are recognisable. The underlying basal unit (225–245 cm), separated by a sharp colour and granulometric variation, consists of homogenous and massive dark brown silty sand, in which X-ray analysis revealed the presence of a freshwater gastropod (*Viviparus contectus*). The conventional ^{14}C age for this mollusc shell is reported to be 9610±40 yr BP, whereas, for the sedimentary OC, ^{14}C ages from selected depths increase from 4020±30 to 9140±40 yr BP downcore.

Core GT2, recovered from the prodelta zone of the Isonzo river mouth, contains the three major stratigraphic units already reported for GT1, although with some differences due to its proximity to the fluvial source. The upper section of the core (0–175 cm) is composed of olive brown silty clay to clayey silt, highly hydrated (47.2% average water content) and weakly bioturbated only at the top. Shelly fragments and complete bivalves and gastropods (*Turritella* sp.) are common in the lower section of this unit. The middle unit (175–300 cm) is separated by an evident colour change and grades downwards into dark grey silty sand and sandy silt. The mottled aspect is due to the alternation of sandy and silty-clayey lenses rich in minute plant debris with the colour changing from greenish brown to dark green and, in addition, to black organic rich pockets. Large shelly fragments of marine bivalves (*O. edulis, Pecten*) and gastropods (*Turritella* sp.) are concentrated between 175 and 200 cm depth. The lowermost part of the unit (280–300 cm) shows irregular dark brown peaty lenses within a silty sand matrix. The basal unit (300–320 cm) is defined by a homogenous and sterile dark brown clayey sand layer. The conventional ^{14}C ages of the sedimentary OC found at selected depths were between 3370±40 and 9380±40 yr BP.

Core GT3, from the deep central basin of the gulf, is characterized by a similar, although more compressed, sedimentary sequence. The uppermost section (0–82 cm) of this core is composed of dark clayey silt, highly hydrated at the top (52% average water content), changing into a very firm greenish grey silty clay downcore. Shelly fragments are scattered throughout the unit except between 52 and 60 cm depth where, in a shell-rich layer, *O. edulis*, undetermined marine bivalves and *Serpulidae* sp. are concentrated. The conventional ^{14}C age of the sedimentary OC found at 64 cm depth is 4560±35 yr BP. This section shows a gradational boundary with the underlying unit (82–92 cm) which consists of fossiliferous and well sorted greenish grey silty sand, with abundant *Cerastoderma glaucum* (8810±40 ^{14}C yr BP), *O. edulis* and minute

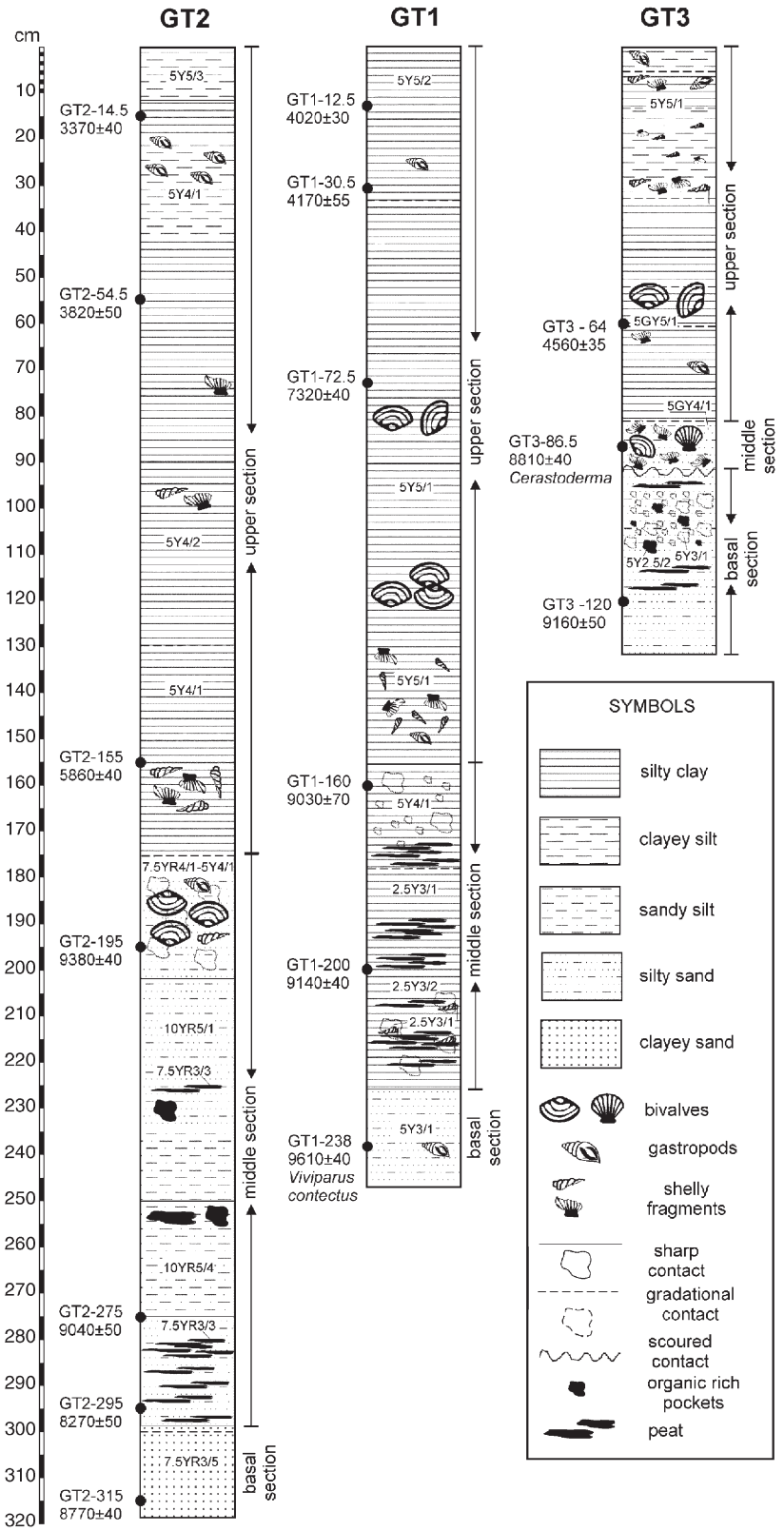

Fig. 2. Core logs of GT1, GT2 and GT3 showing the sedimentary sequence and conventional ^{14}C ages on selected shells and bulk sedimentary OC.

shelly fragments. This unit is underlain with a sharp boundary by the basal core section (92–130 cm) composed of dark, sterile, silty fine sand down to the base. The conventional ^{14}C age obtained from the sedimentary OC at 120 cm depth is 9160±50 yr BP. The abundance of plant debris and peaty lenses gives a mottled aspect due to colour changes from grey to very dark grey.

4.2. Organic carbon, inorganic carbon, $\delta^{13}C_{org}$, nitrogen and sulfur

The upper section of cores GT1 (Fig. 3A), GT2 (Fig. 3B) and GT3 (Fig. 3C) are characterised by rather low organic carbon (OC) and N contents (about 0.6% and 0.12%, respectively), except for higher values at the top of the cores (1.10–1.31% for OC and 0.16–0.23% for N). The C/N ratios range from about 4 to more than 8 in cores GT1 and GT3, whereas they are higher (between 8 and 10) in core GT3. Inorganic carbon (IC) increases slightly downcore from 3.72% to 6.13% following the progressive increase of the sandy component in the sediment of all three cores. $\delta^{13}C_{org}$ values are constant and typically marine in the first 60 cm (average −21.9±1.0‰), from where the isotopic composition clearly starts decreasing downcore to more negative values of −25.7‰.

In the following middle section of core GT1, the sharp increase of OC values from 1.90% to 4.33% and N contents from 0.20% to 0.31%, C/N ratios (11.3–16.0) and the mean $\delta^{13}C_{org}$ value (−26.7±0.2‰) suggest that most of the organic matter present in lenses is of terrigenous origin. The $\delta^{13}C_{org}$ value still decreases in the upper part of the middle section of core GT2, following the trend described in the previous section, from −24.5‰ to −27.4‰, remaining relatively uniform in the section down to the base. In the basal part of the section, a slight increase is observed for OC and N contents and C/N ratios showing maxima of 1.67%, 0.14% and 13.8%, respectively. The IC contents, ranging from 6.50% to 8.05%, reflect the variability of the silty sandy component of carbonate origin in the sediments. A fossiliferous silty sand layer characterizes the middle section of core GT3, showing slightly higher values of OC (1.88%) and IC (6.52%) than the upper section, a lower content of N (0.06%) and a high C/N ratio (36.6).

The bottom sedimentary section in core GT1 is characterised by a relatively low OC value (0.6%) and medium N content (0.22%), whereas the maximum IC content (8.81%) is due to the prevalence of the carbonate sand component. The C/N ratio of 5.9, comparable with the upper core section, and $\delta^{13}C_{org}$ value of −26.9‰ fall into the range for lacustrine organic matter (Meyers, 1997). Results obtained for the basal section of core GT2 are of the same magnitude as those previously observed for the middle section. High contents of OC (up to 4.35%) and C/N ratios (46.1) are observed in the upper part of the last section of core GT3 where peaty lenses and pockets of organic matter can be seen. IC contents are the highest in the core (6.58–7.33%), except for the organic rich level at 109–110 cm depth, whereas N contents and $\delta^{13}C_{org}$ values are generally constant over the section, the latter having the most negative values (averaging −26.1±0.4‰) in the whole core.

The distribution of total S in the cores shows characteristic features, with higher contents in the surface layers (0.29% GT1; 0.33% GT2; 0.37% GT3) that slightly decrease in the first 50 cm down to about 0.10–0.15% in the lower sections. A significant increase is observed in core GT1 for the middle section, where a maximum of 0.95% S is reached, probably caused by the presence of metal sulfides in reduced sediments as also indicated by higher concentrations of organic matter due to peaty lenses in the sediments.

4.3. Calcium, magnesium, aluminum, iron and titanium

The distribution of Ca and Mg in cores GT1 (Fig. 3A) and GT2 (Fig. 3B) is related to the abundance of carbonates in the coarser, silty sand fraction of the sediments, showing increasingly higher contents in the lower sections. In core GT1, Ca increases from about 9%, at the top layer, to about 14% in the lower part of the upper section, with a decrease in the more organic sediment of the middle section (9%), to reach the highest content in the coarser basal part (22.8%). The Mg trend increases linearly from the surface down to the basal part of the upper section (2.0–3.5%) remaining constant over the rest of the core. The relationship between Ca content and grain-size variability is more evident in GT2, ranging from 8.2% to 16.7% in the upper section and reaching a constant value of 18.6±1.6% in the lower sections.

In all three cores, the profiles of Al, Fe and Ti are strongly correlated with the clay fraction of sediments. A decreasing trend is detectable in core GT1 (Fig. 3A), down to the upper limit of the middle section, followed by a slight increase in values due to finer grain-size (Al: 7.35–1.71%; Fe: 2.56–0.83%; Ti: 0.59–0.13%), whereas the lowest contents are related to the sandy layer at the core bottom. The decreasing trend of the three elements in core GT2 (Fig. 3B) from the topmost layers down to 240 cm depth, where the lowest contents (Al: 2.05%; Fe: 0.89%; Ti:

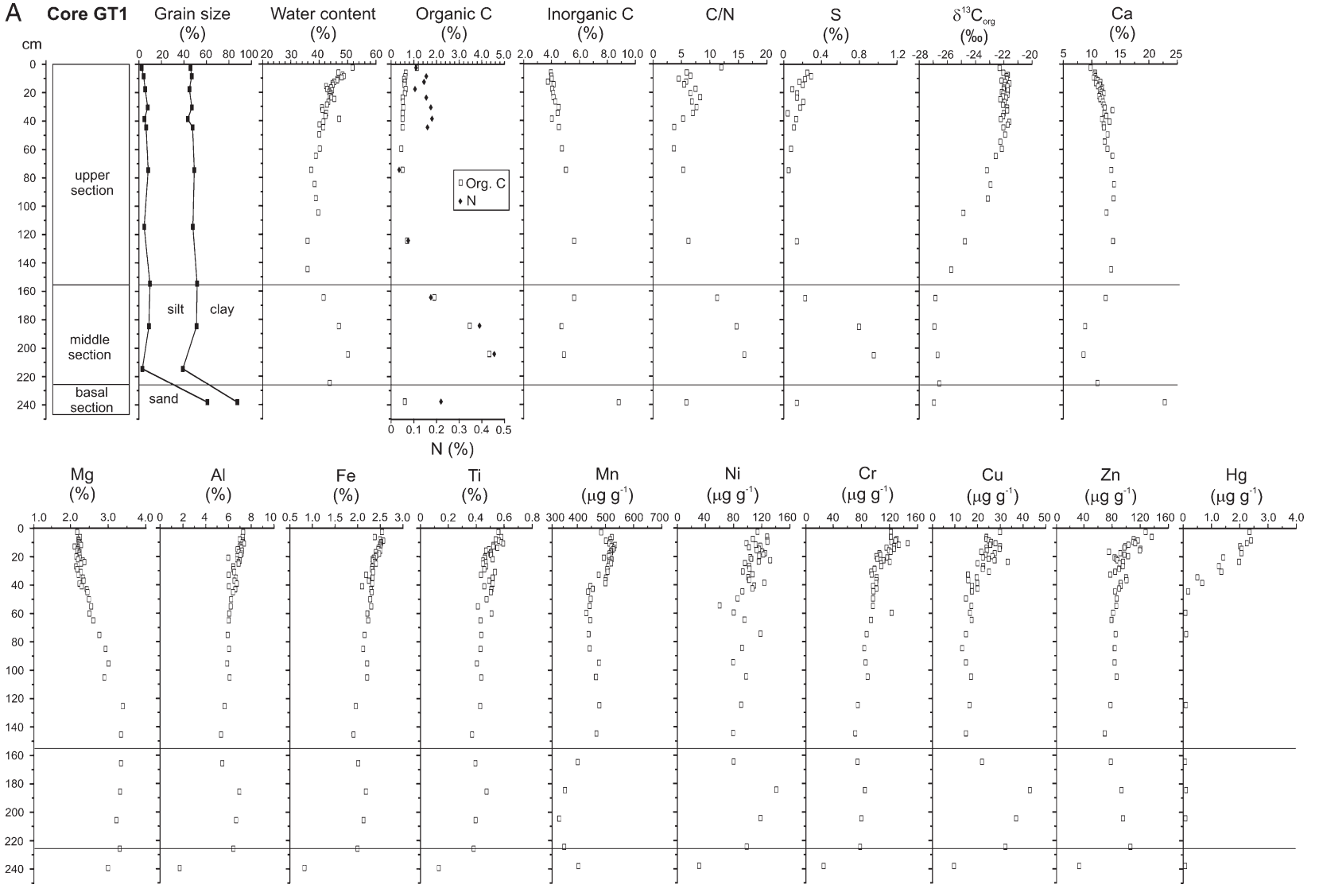

Fig. 3. (A) Vertical profiles of grain-size, water content, major and trace elements and $\delta^{13}C_{org}$ in core GT1. (B) Vertical profiles of grain-size, water content, major and trace elements and $\delta^{13}C_{org}$ in core GT2. (C) Vertical profiles of grain-size, water content, major and trace elements and $\delta^{13}C_{org}$ in core GT3.

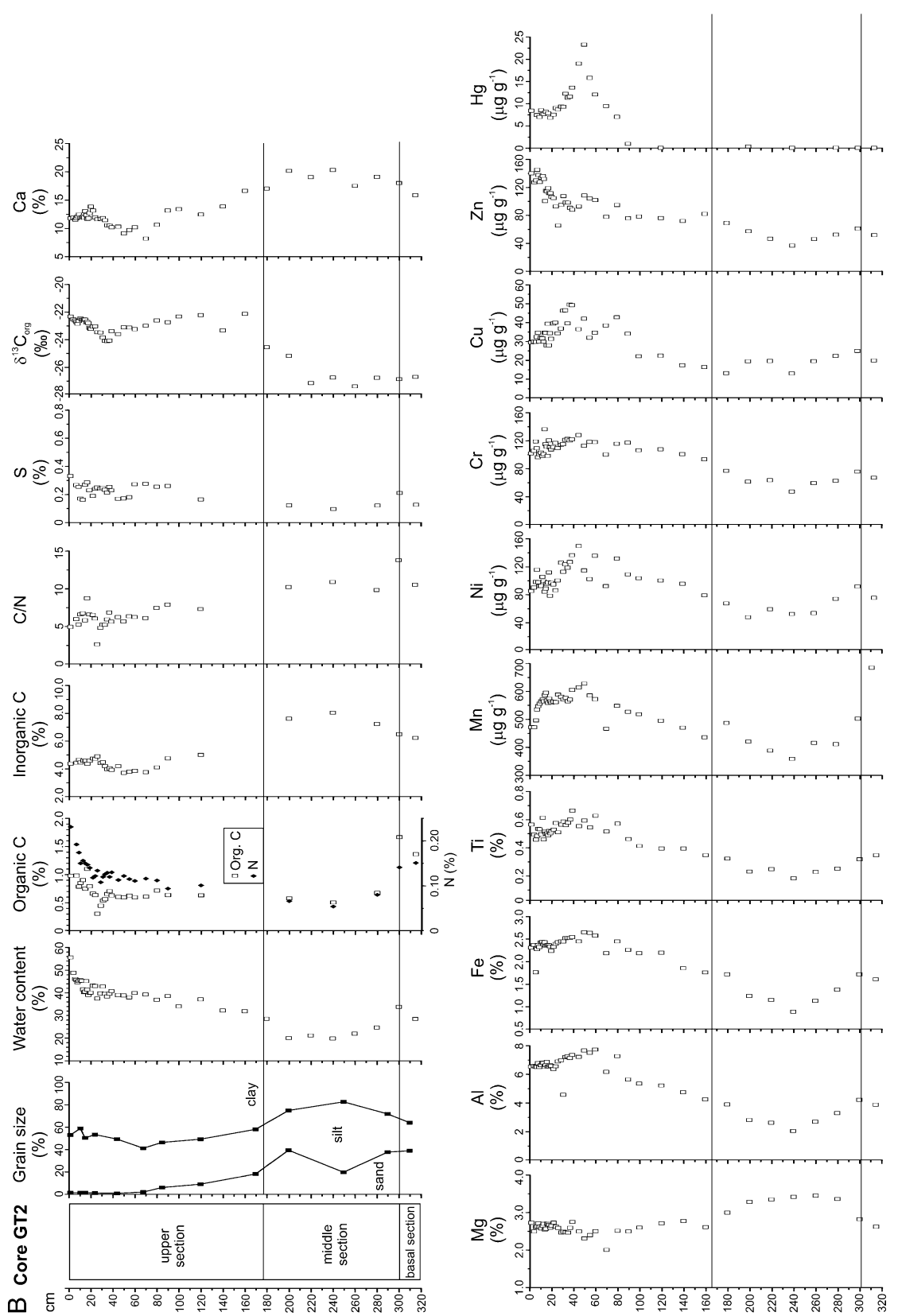

Fig. 3 (*continued*).

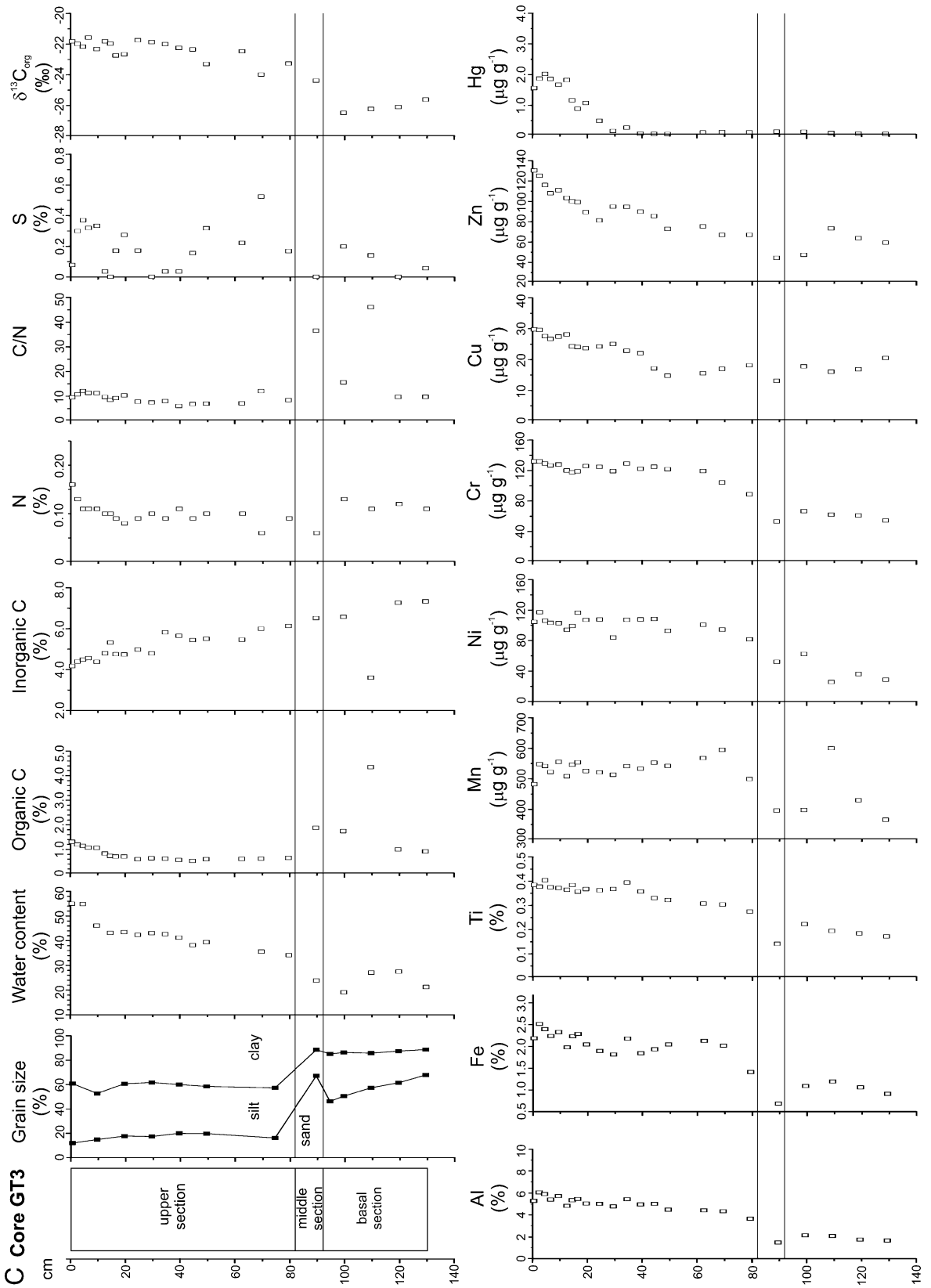

Fig. 3 (*continued*).

0.18%) are found, is interrupted by a peak between 50 and 60 cm depth (Al: 7.74%; Fe: 2.65%; Ti: 0.63%). In the basal part of the core, values increase according to clay content variability. In core GT3 (Fig. 3C), a progressive linear decrease of the three elements from the top of the core to the basal section is observed, with minima related to the sandy silty layer at a depth of 82–92 cm corresponding to the middle section (Al: 8.55–3.98%; Fe: 3.71–1.19%; Ti: 0.40–0.14%).

4.4. Manganese, nickel, chromium, copper, and zinc

Down-core distributions of these heavy metals suggest a highly significant relationship among them and with those elements (Al and Fe) that are the major constituents of aluminosilicates in the finer silty-clayey fraction of the sediments. In core GT1 (Fig. 3A), Mn, Ni, Cu, Cr and Zn profiles show a slight decrease from the top of the core (Mn: 534–431 μg g^{-1}; Ni: 132–60 μg g^{-1}; Cu: 13–33 μg g^{-1}; Cr: 71–146 μg g^{-1}; Zn: 70–136 μg g^{-1}) to the lower limit of the upper section. Concentrations of Cr and Zn remain almost constant in the middle section, whereas an apparent enrichment is observed for Ni and Cu (up to 141 and 43 μg g^{-1}, respectively). Conversely, the Mn content is noticeably reduced (down to 336 μg g^{-1}). The lowest concentrations of heavy metals are found in the basal and more sandy section of the core.

In core GT2 (Fig. 3B), the heavy metals follow three distinct trends: a slight increase from the top layers down to 50–60 cm depth is observed (up to 628 μg g^{-1} Mn, 150 μg g^{-1} Ni, 128 μg g^{-1} Cr, 50 μg g^{-1} Cu), except for Zn, which, on the contrary, decreases from 145 to about 90 μg g^{-1}. A sharp decrease is then evident down to 240 cm depth, where the lowest contents (359 μg g^{-1} Mn, 48 μg g^{-1} Ni, 47 μg g^{-1} Cr, 13 μg g^{-1} Cu, 37 μg g^{-1} Zn) are reached. In the basal part of the core, values increase according to grain-size variability.

Almost constant values of Mn, Ni and Cr (averaging 536, 102 and 121 μg g^{-1}, respectively) are present in the upper section of core GT3 (Fig. 3C), decreasing slightly in the proximity of the middle section, following the coarsening of grain-size downwards. Zn and Cu trends show a linear decrease from the top of the core (130 and 30 μg g^{-1}, respectively) to the basal section for the former (44 μg g^{-1}), and down to 50 cm depth for the latter (about 15 μg g^{-1}).

4.5. Mercury

The profiles of Hg content in all three cores show a peculiar trend, clearly reflecting a contamination process that has affected the more recent history of the coastal area and has been well recorded in the marine sediments. In cores GT1 (Fig. 3A) and GT3 (Fig. 3C), more distant from the riverine source, an exponential decrease is observed from the top layers (2.4 and 2.02 μg g^{-1}, respectively) down to about 40 cm depth where Hg concentrations reach almost constant values corresponding to natural background levels. These are estimated to be between 0.04 μg g^{-1} (Ogorelec et al., 1981) and 0.10 μg g^{-1} (Faganeli et al., 1991) for the southern sector of the Gulf and 0.17 μg g^{-1} for the western part of the study area (Covelli et al., 2001). Unlike the previous cores, Hg contents in GT2 (Fig. 3B) show an increasing, nearly exponential, trend from the surface (8.45 μg g^{-1}) to about 50 cm depth, where a concentration peak of 23.32 μg g^{-1} is reached. From that depth, the metal abundance decreases, also nearly exponentially, down to background values reached at about 100-cm depth. A similar trend and apparent peak at 16–19 cm depth were already found in a 70-cm-long core (AA1 in Fig. 1) collected 4.5 miles south–east of the river mouth. Here, they were considered to be related to cinnabar ore extraction activity at the Idrija mine (Covelli et al., 2001).

5. Discussion

5.1. The Holocene stratigraphic sequence

Holocene sedimentation processes in the northern Adriatic Sea started with a sea-level rise, dated back to 18 ka, after the last glaciation. This rise was initially very rapid, about 10 mm yr^{-1}, up to 6 ka (Amorosi et al., 1999) followed by a phase of high-stand corresponding to the last 6000 yr, when the rate would have decreased to about 0.5 mm yr^{-1} (Preti, 1999). As a consequence of the high-stand conditions, through the littoral dispersion of the coastal sediments, an almost uninterrupted system of lagoons (from west to east, the Venice, Caorle and Marano lagoons) developed along the northern coastal stretch from the Po river to the Isonzo river (Bortolami et al., 1977; Marocco, 1991). North of the Po river delta, the Adriatic shelf has been defined as sediment starved during high-stand conditions (Trincardi et al., 1994; Correggiari et al., 1996a). The present surface deposits on the shelf consist of a few metres thickness of muddy prodelta wedges close to the major riverine sources. Between Venice and Trieste, residual continental morphological features such as terraces, mounds, ridges and channels, associated with different depositional environments (paleodeltas, ancient shorelines and lagoonal deposits) were recognised on the shelf

(Mosetti, 1966; Brambati and Venzo, 1967; Rossi et al., 1968).

The present hypothesis about sea-level rise in the Gulf of Trieste is mostly based on recent research in the central and southern Slovenian sector of the study area (Ogorelec et al., 1984, 1991, 1997). Six boreholes were drilled along the inner part of the shallow Koper and Piran bays, which are submerged valleys of the small rivers flowing through the Istrian Peninsula. The boreholes were drilled to depths ranging from about 40 to 60 m, reaching the Eocene flysch basement, and revealed an alternation of marine, brackish and fluvial facies. The oldest Holocene sediments were recovered from borehole MK-6 in the inner part of Koper bay at a depth of 48 m below the present sea level (Ogorelec et al., 1991, 1997) and date back to ca. 11 ka according to the sea-level history curves of Fairbanks (1989, 1990). Further south in Piran bay, a peat layer found at 26.5 m depth in the borehole V-6 and dated by ^{14}C radiodating to 9180±120 yr BP is overlaid by a quite homogeneous marine-brackish depositional sequence (Faganeli et al., 1987). The marine ingression in the Gulf of Trieste during the Holocene would have affected the Istrian coast about 10,000 yr BP and more recently the Venetian-Friulian paleoplain.

Conventional ^{14}C ages of bulk sedimentary OC in the basal part of the two cores, 9030±70 and 9140±40 yr BP for GT1, and 9160±120 yr BP for GT3 correspond with the age reported for the peat layer in the V6-borehole. The very low $\delta^{13}C_{org}$ values and higher C/N ratios supported by stratigraphic features (dark brown clays and peats) suggest that these sections were formed in low energy environments influenced by freshwater inputs and abundant vegetation, such as swamps or alluvial plains, developed just before the marine transgression. This hypothesis is supported by the age of 9610±40 yr BP for a gastropod (*V. contectus*), typical of lacustrine environment, found at the bottom of core GT1. Detailed micropaleontological investigation (Melis, unpublished data) revealed that the basal sediments are almost sterile except for frequent gyrogonites from *Characeae.*

Similar paleoenvironmental conditions were reached slightly later at the shallower (−15 m depth) GT2 location, considering the basal datings of 8270±50 and 8770±40 yr BP. These results are consistent with the Early Holocene age/depth model for the northern Adriatic Sea (Correggiari et al., 1996b; Amorosi et al., 1999; Preti, 1999). According to this interpretation the oldest datings of GT2 (9380±40 at −195 cm and 9040±50 at −275 cm) measured above the two basal ^{14}C samples were considered not reliable.

Paleoenvironmental studies of the foraminiferal assemblages of the GT3 core sections, based upon previous work in the area (e.g. Serandrei Barbero et al., 1989; Albani and Serandrei Barbero, 1990), indicate a subsequent gradual evolution to a paralic system, as testified by the abundant typical lagoon/estuarine bivalves (*C. glaucum*) found between 82 and 92 cm depth and dated to 8810±40 ^{14}C yr BP. Evidence of the development of a rapid marine transgression comes also from the relative increase of typical or exclusive marine foraminifera species in the sedimentary sequence.

In the uppermost marine sections of the cores, the age of bulk sedimentary OC does not show any relevant change with depth to about 60 cm. In contrast, using Hg as a recent geochronological tracer in core GT2, the sediment layer at 55 cm could date to 1913 by correlation with mining activity (see Fig. 8 and Covelli et al., 2001). The apparent discrepancy between the sediment chronology and the older ^{14}C ages of bulk sedimentary OC at the same depth suggests that a significant fraction of sedimentary OC could be relatively old and most likely of partly allochthonous origin. In recent work (Ogrinc et al., 2005), it was reported that radiocarbon analyses of sedimentary OC yield depleted Δ^{14}C values (−338.7‰ to −429.4‰), indicating a significant fraction of relatively old OC. As a consequence, the natural abundance of ^{13}C and ^{14}C tracers suggests a two-component mixture of ancient and modern C in the sediments down to approximately 60 cm sub-bottom, with an estimated ≈45% of sedimentary OC probably being derived from ancient sedimentary OC (kerogen).

5.2. Geochemistry

Both Al and Fe show strong positive correlations with mud contents (Al=0.770; Fe=0.627, $p \leq 0.001$) as a reflection of their coexistence in the crystalline structure of fine grained aluminosilicate minerals. The high negative correlations of Al with IC ($r=-0.751$), Mg ($r=-0.624$) and especially with Ca ($r=-0.917$) is explained by the detrital, and to a lesser degree biogenic, carbonate component which mainly affects the coarser sandy fraction of the sediment in the gulf (Ogorelec et al., 1991). The positive correlations of Ti ($r=0.619$), Cr ($r=0.845$), Ni ($r=0.735$), Cu ($r=0.435$) and Zn ($r=0.699$) with Al confirm that Al can be the ideal reference element and suggest that these trace metals are mostly held in the clay minerals. Among the trace metals, Hg is the only one showing a less significant correlation ($r=0.293$) with Al. If plotted against the main grain-size components, Hg shows the best

Table 1
R-mode Varimax rotated factor matrix for geochemical parameters

	Factor 1	Factor 2	Factor 3	Factor 4	Communality
Clay	0.968	−0.004	0.011	0.031	0.938
IC	−0.966	−0.006	−0.228	0.023	0.986
Fe	0.933	−0.007	0.316	0.042	0.972
Al	0.931	0.113	0.304	0.040	0.974
Ca	−0.918	−0.265	−0.191	0.033	0.951
Ti	0.893	0.024	0.383	−0.056	0.948
Mud	0.877	0.042	0.401	0.169	0.960
Ni	0.838	0.191	0.028	−0.107	0.751
Cr	0.838	−0.131	0.440	−0.082	0.920
Mg	−0.649	0.552	−0.028	0.286	0.808
Zn	0.618	0.104	0.576	0.237	0.781
OC	0.013	0.965	−0.157	0.011	0.956
S	0.191	0.903	0.111	0.058	0.868
Ntot	0.025	0.864	0.127	0.126	0.779
Hg	0.192	−0.070	0.837	−0.335	0.855
Silt	0.420	0.093	0.817	0.306	0.946
Cu	0.469	0.447	0.557	−0.276	0.806
Mn	−0.003	−0.154	0.046	−0.883	0.806
Eigenvalues	8.694	3.185	2.85	1.275	
Total variance	48.297	17.695	15.833	7.084	

correlation with silt (r=0.551) supporting the hypothesis that particles between 53 and 2 μm, and particularly those between 16 and 2 μm (Covelli et al., 2001), are the most important metal-carriers in the gulf.

5.2.1. Factor analysis

Principal Component Analysis (PCA) using VARIMAX rotation was applied to investigate the interrelationships between the variables. Four main factors explain almost 88.9% of the total variance (Table 1) in the compositional features of the samples. Factor 1 accounts for 48.3% of the variance and shows significant high loadings (>0.84) of Fe, Al, Ti, Ni and Cr, lesser loadings of Zn (0.64) as well as mud and clay components, whereas negative high loadings of Ca, IC and Mg are related to carbonates mostly present in the coarser fraction of the sediment. The first Factor reflects the natural composition of sediments due to the accumulation of terrigenous material composed of carbonates and silicates. The trace metal variability can be explained by grain-size and mineralogical variations throughout the cores. Factor 2 accounts for 17.7% of the variance, comprising high loadings of OC, S and N, which are mostly related to the organic matter present in the peaty lenses in the deepest sections of the cores. Factor 3 accounts for 15.8% of the variance where Hg, the factor end member, is positively correlated with silt and Cu, and partially with Zn. This factor represents anthropogenic perturbation in the most recent history of the gulf due mainly to the mining of cinnabar ore with possibly associated Cu and Zn sulfides. Factor 4 is only represented by Mn and accounts for 7.1% of the variance and for which there is no obvious explanation.

5.2.2. Cluster analysis

Cluster analysis was performed on the basis of the values of 19 standardized variables using Ward's hierarchical agglomerative method and Euclidean distance measures. Fig. 4 shows the dendrogram produced by clustering 112 subsamples of the three cores. The samples fall into four main groups (A, B, C and D) that have a clear stratigraphic meaning (Table 2 and Fig. 5). Cluster A includes the basal sections of all three cores, representing the uppermost part (Early Holocene) of the transgressive system tract recognized by Trincardi et al. (1994), Correggiari et al. (1996a) and Fabbri et al. (2001). This group is characterized by the highest contents of sand, IC, Ca and Mg, with all the remaining variables being very low except for OC, which averages about 1%. The B group, which is close to the A group, comprises the middle section of all three cores related to Holocene deposition. This group can be

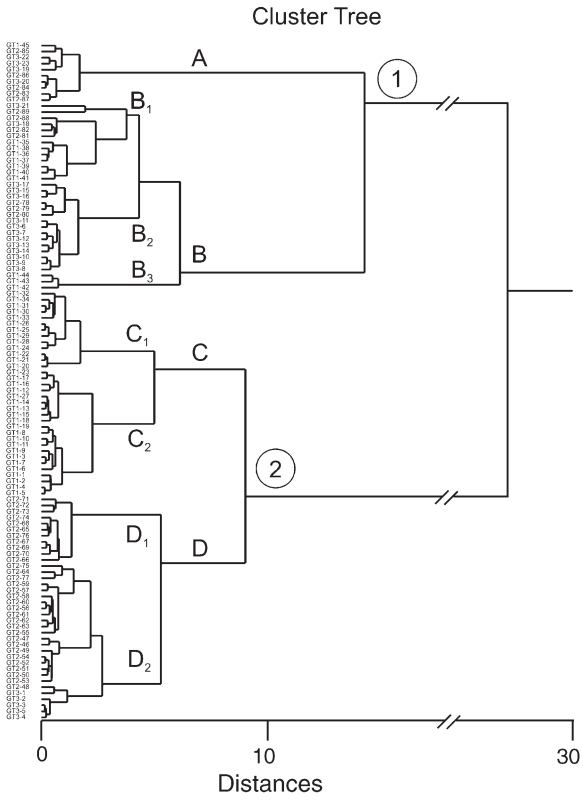

Fig. 4. Dendrogram obtained by cluster analysis (Euclidean distance and Ward linkage).

Table 2
Descriptive statistics for variables of the main clusters

	Cluster	A	B1	B2	B3	C1	C2	D1	D2
Corg (%)	avg.	0.99	1.59	0.65	3.90	0.49	0.63	0.61	0.88
	range	0.51–1.88	0.50–4.35	0.53–0.83	3.47–4.33	0.45–0.52	0.50–1.13	0.45–0.72	0.31–1.31
	std	0.54	1.33	0.08	0.61	0.03	0.17	0.08	0.25
Cinorg (%)	avg.	7.43	5.54	5.25	4.81	4.50	4.02	4.07	4.50
	range	6.52–8.81	3.61–6.50	4.74–6.00	4.72–4.90	4.28–4.75	3.47–4.52	3.72–4.49	3.77–4.91
	std	0.75	0.98	0.43	0.13	0.20	0.26	0.25	0.25
Ntot (%)	avg.	0.07	0.12	0.07	0.30	0.32	0.11	0.12	0.14
	range	0.03–0.12	0.04–0.20	0.03–0.10	0.28–0.32	0.08–0.88	0.07–0.15	0.11–0.13	0.09–0.23
	std	0.03	0.05	0.02	0.03	0.38	0.02	0.01	0.04
S (%)	avg.	0.09	0.15	0.16	0.87	0.11	0.19	0.22	0.26
	range	0.00–0.20	0.05–0.23	0.00–0.52	0.80–0.95	0.04–0.21	0.09–0.29	0.17–0.27	0.08–0.37
	std	0.07	0.06	0.15	0.11	0.07	0.06	0.04	0.07
Al (%)	avg.	3.22	5.18	6.97	6.68	6.34	6.96	7.09	6.87
	range	1.71–4.62	3.88–6.14	4.76–7.95	6.43–6.94	6.01–6.88	5.97–7.35	4.58–7.74	5.65–8.55
	std	1.00	0.88	1.02	0.26	0.28	0.32	0.86	0.70
Ca (%)	avg.	19.84	14.61	13.27	9.44	12.49	11.22	10.57	12.06
	range	17.53–22.80	12.42–18.03	12.49–13.90	8.53–10.98	11.47–13.60	9.79–12.24	9.13–11.84	8.21–13.86
	std	1.76	1.93	0.72	1.34	0.65	0.64	0.82	1.07
Mg (%)	avg.	3.31	2.98	2.70	3.28	2.37	2.23	2.50	2.60
	range	3.00–3.45	2.61–3.39	2.60–2.77	3.22–3.32	2.15–2.60	2.11–2.37	2.31–2.75	2.01–2.73
	std	0.16	0.28	0.09	0.05	0.15	0.06	0.11	0.15
Fe (%)	avg.	1.24	1.98	3.00	2.10	2.27	2.44	2.53	2.55
	range	0.83–1.59	1.61–2.61	1.86–3.49	2.00–2.18	2.10–2.41	2.32–2.56	2.45–2.65	1.77–3.71
	std	0.26	0.28	0.50	0.10	0.08	0.08	0.08	0.51
Ti (%)	avg.	0.20	0.36	0.36	0.42	0.47	0.52	0.59	0.49
	range	0.13–0.25	0.19–0.44	0.30–0.41	0.38–0.47	0.41–0.52	0.45–0.59	0.55–0.66	0.37–0.61
	std	0.04	0.07	0.03	0.05	0.03	0.04	0.03	0.06
Mn (ppm)	avg.	399	514	532	348	471	514	584	544
	range	359–430	401–979	471–595	336–356	431–520	485–534	549–628	467–595
	std	23	147	30	11	32	12	23	37
Cr (ppm)	avg.	56	79	118	81	101	118	119	113
	range	26–67	62–94	101–129	78–85	94–123	94–146	113–128	96–136
	std	12	10	9	4	8	13	4	12
Ni (ppm)	avg.	50	82	101	119	95	115	125	98
	range	29–74	26–118	84–116	99–141	60–109	93–132	103–150	79–117
	std	14	21	8	21	14	11	13	10
Cu (ppm)	avg.	17	17	21	37	18	26	41	32
	range	10–22	13–25	15–28	32–43	15–23	20–33	32–50	27–40
	std	4	3	4	5	2	3	6	4
Zn (ppm)	avg.	49	75	85	98	89	102	98	115
	range	33–64	52–86	67–103	93–106	77–100	76–136	88–108	65–145
	std	10	10	12	7	7	16	7	20
Hg (ppm)	avg.	0.138	0.094	0.496	0.088	0.504	1.853	13.167	5.938
	range	0.072–0.410	0.063–0.119	0.064–1.823	0.078–0.098	0.080–1.258	0.672–2.395	7.047–23.321	0.986–9.493
	std	0.114	0.018	0.565	0.014	0.534	0.543	4.682	3.184
Sand (%)	avg.	57.87	23.79	16.71	5.98	6.42	5.01	3.45	4.93
	range	39.45–67.87	4.65–57.36	9.04–20.04	3.04–8.91	6.42	2.45–7.87	0.88–6.02	1.13–14.91
	std	10.96	23.25	4.03	4.15	–	1.98	3.63	5.91
Silt (%)	avg.	27.69	35.96	41.18	39.14	41.33	40.61	44.44	47.99
	range	20.84–35.77	25.12–43.32	38.72–44.26	35.99–42.28	41.33	38.47–43.47	40.36–48.51	37.88–57.47
	std	6.58	8.51	2.05	4.45	–	2.29	5.76	7.10
Clay (%)	avg.	14.44	40.25	42.11	54.89	52.25	54.38	52.12	47.07
	range	11.30–25.07	14.21–52.03	38.28–50.74	48.81–60.97	52.25	52.94–56.64	50.61–53.62	39.15–58.82
	std	5.28	15.90	4.51	8.60	–	1.55	2.13	6.36
Mud (%)	avg.	42.13	76.21	83.29	94.03	93.58	94.99	96.55	95.07
	range	32.13–60.55	42.64–95.35	79.96–90.96	91.09–96.96	93.58	92.13–97.55	93.98–99.12	85.09–98.87
	std	10.96	23.25	4.03	4.15	–	1.98	3.63	5.91

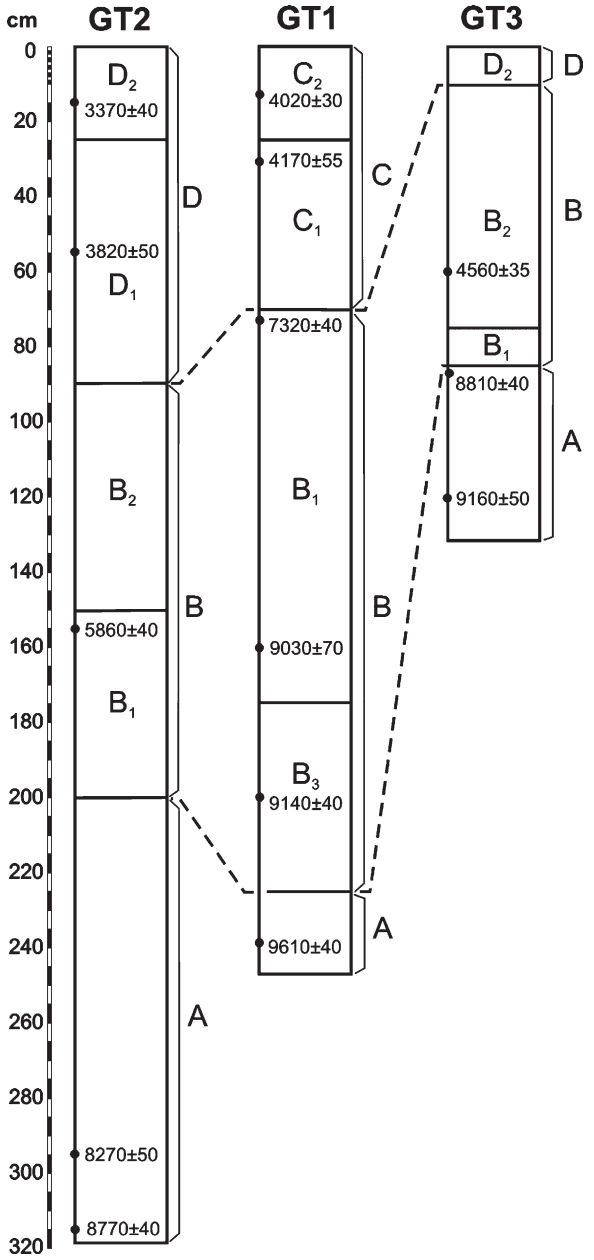

Fig. 5. Correlations among core sections on the basis of cluster analysis results.

easily separated into three subgroups (B1, B2 and B3). The most distinctive of the three subgroups is B3, corresponding to the 175–225 cm section in core GT1 where visual inspection shows high concentrations of organic matter as peat accumulated in lenses. This section consists of fine material (about 94% of mud) with very high contents of OC (about 4%), N, S and Mg and high concentrations of Al, Ni, Cu and Zn which can be explained, for the last two elements, by the formation of authigenic sulfide minerals. These results, along with highly negative $\delta^{13}C_{org}$ values, indicate the deposition of sediments belonging to lacustrine or swamp sedimentary environments in the eastern part of the gulf, affected by freshwater inputs from the pre-transgression drainage system involving the present secondary streams flowing into the gulf from the Istrian Peninsula (Rosandra, Ospo, Rizana and Dragonja rivers). The subgroups B1 and B2 testify to the gradual deepening of the marine environment due to marine transgression. Differences in terms of composition between the B1 and B2 groups are due to higher contents of OC, N, Ca, Mg and sand and lower concentrations of Al, Fe, Cr, Ni, Cu, Zn and silt in B1 in comparison with the B2 group (Table 2). It is worth noting the absolute correspondence between the sedimentary horizons belonging to the B1 group and the three core sections where the increase of $\delta^{13}C_{org}$ values occurs (Fig. 3A, B and C), testifying to the transition from continental to marine conditions. Similar deposits, affected by inputs of organic and terrigenous material of fluvial origin, were accumulated during the rapid Holocene transgression up to about 6000 yr BP. Conversely, the B2 facies suggests a typical marine depositional environment characterized by fining upwards material of fluvial origin which would represent sedimentation that occurred in the western gulf area after the maximum marine transgression, corresponding with the highstand system tract of Trincardi et al. (1994). The lack of cluster B2 in core GT1, along with a major thickness of facies B1 at this site, seems to indicate a longer period of intermediate conditions here, far off from the main terrigenous input of the Isonzo river. According to Marocco (1991), the Isonzo river paleodelta was located further west of Grado in the Roman age. The formation of the lagoon environment west of Grado was due to a progressive migration of the river mouth eastwards and consequent increase in the subsidence of the former alluvial plain. Only in more recent times (9th–18th centuries AD) did the Isonzo river reach the coastal area between Grado and the present river mouth. This event contributed to the recent increase in the sedimentation rate in the gulf area, especially in the western part. Taking into consideration Hg as a geochronological tracer, clusters C and D and the following subgroups, C1,C2 and D1, D2, represent the modern deposits accumulated in the last thousand years in the prodelta zone of the Isonzo river. The deposits are of very fine sediments, showing a recent increase of the silt/clay ratio at the top of cores GT2 and GT3 (cluster D2). Almost all metals show higher average concentrations in cluster D1, and secondarily in D2 and C2 due to the influence of

anthropogenic inputs primarily involving Hg, but subordinately Cu and Zn.

These findings are consistent with the metal distributions in surficial sediments of the Gulf of Trieste (Covelli and Fontolan, 1997). The metals are more related to mineralogical composition than to anthropogenic sources with the only exception being Hg. Relationships between trace elements and the finest fraction of sediment particles (<2 μm) confirm their lithogenic provenance influenced by fluvial inputs from the Isonzo river.

5.3. Baseline and enrichment factors

According to the literature (Schropp et al., 1990; Loring, 1990, 1991), before any examination of enrichment, a normalization to a reference element is necessary to compensate for grain-size and mineralogical effects on the metal variability in samples. A first attempt at regional geochemical normalization using regression lines of trace metals on a normalizing or conservative element (i.e. Al, Li, Fe, etc.) was previously made on surface sediment samples of the studied area by Covelli and Fontolan (1997). The study pointed out how this procedure seems to be most suitable in determining regional baseline functions and, subsequently, in calculating enrichment factors as simple ratios between real and theoretical values (Colizza et al., 1996). In the present study, the availability of subsurface samples from long cores allowed this procedure to be applied not only to present and pre-industrial time (i.e. ca. 200 yr) sediments, but also to the whole Holocene (ca. 10,000 yr).

Simple linear regressions versus Al were initially performed on all core levels and the results were plotted along with the 95% prediction limits (Fig. 6). Data points falling outside the two 95% predictions limits, delineating the expected natural range, were considered to be anomalous and removed from the original data set. Metal-Al linear relationships were recalculated for the samples statistically belonging to the natural population of marine sediments of the Gulf of Trieste (Table 3). These regression lines, along with prediction limits can be used to assess if sediments are enriched with metals on a regional scale, i.e. in the Gulf of Trieste. Concentrations that are higher than the prediction limits can be a consequence of contamination and an unusual amount of metal-bearing minerals (Loring, 1991), and to the onset of trace metals remobilization during early diagenesis (Berner, 1980; Lapp and Balzer, 1993; Skowronek et al., 1994). The degree of enrichment (or enrichment factor EF) can be given by the ratio between the measured concentration and the predicted metal value determined through the linear functions of Table 3. If we consider single cores, the possible alterations of the natural composition of marine sediments due to anthropogenic sources with time can be evaluated. The vertical profiles of metal EFs (Fig. 7) show that Fe, Mn and Ti are not affected by anthropogenic enrichment, but are bound in the crystalline structure of minerals. The EF distribution with depth is relatively uniform for Cr and Ni. Zn appears to be slightly enriched at the top of the three cores especially in the first 20 cm (GT1 EF = 1.3, GT2 EF = 1.50; GT3 EF = 1.57). Cu shows significant enrichment only in core GT2, between 10 and 90 cm sediment depth. This enrichment approximately matches the interval of high Hg content as reported below. If surficial enrichments are due to anthropogenic sources, mainly through fluvial inputs, local enrichments of metals in the deeper core sections are probably related to post-depositional processes with the formation of authigenic minerals. Pyrite as large framboids (up to 200 μm), formed during early diagenesis in reduced conditions, was found to be <5% of the total sediment in the small bays along the southern coast of the gulf (Ogorelec et al., 1991) as well as in the basal section of core GT3 (Melis, personal communication).

Hg was the only metal showing a correlation with Al significant at a lower level ($p \leq 0.05$–0.001) since sedimentary deposits at the core tops show extremely high concentrations of this metal due to mining residues. Conversely, Hg values in the deepest core sections are relatively constant and slightly lower than the preliminary estimated background, or pre-mining activity value, of 0.17 μg g^{-1} reported by Covelli et al. (2001). The statistical approach described for other metals could not be applied for Hg because if samples with high concentrations are removed from the scatterplot, the linear correlation with aluminium is poorly defined. The Hg baseline was therefore considered as an average of concentrations in the basal levels of the cores (0.13 μg g^{-1}). Hg contents were normalized to Al but little change was produced in the shape of Hg concentration versus depth profiles. This fact indicates that peaks and lows are not a consequence of grain-size variations. The EF for Hg was calculated as $Hg/Al_{(sample)}/Hg/Al_{(baseline)}$. The degree of Hg enrichments, in the core tops, appears to depend on the distance from the fluvial source (GT1 EF = 16.8; GT2 EF = 27.2; GT3 EF = 7.5). However, maximum enrichments were achieved in the recent past, since they are recorded in the

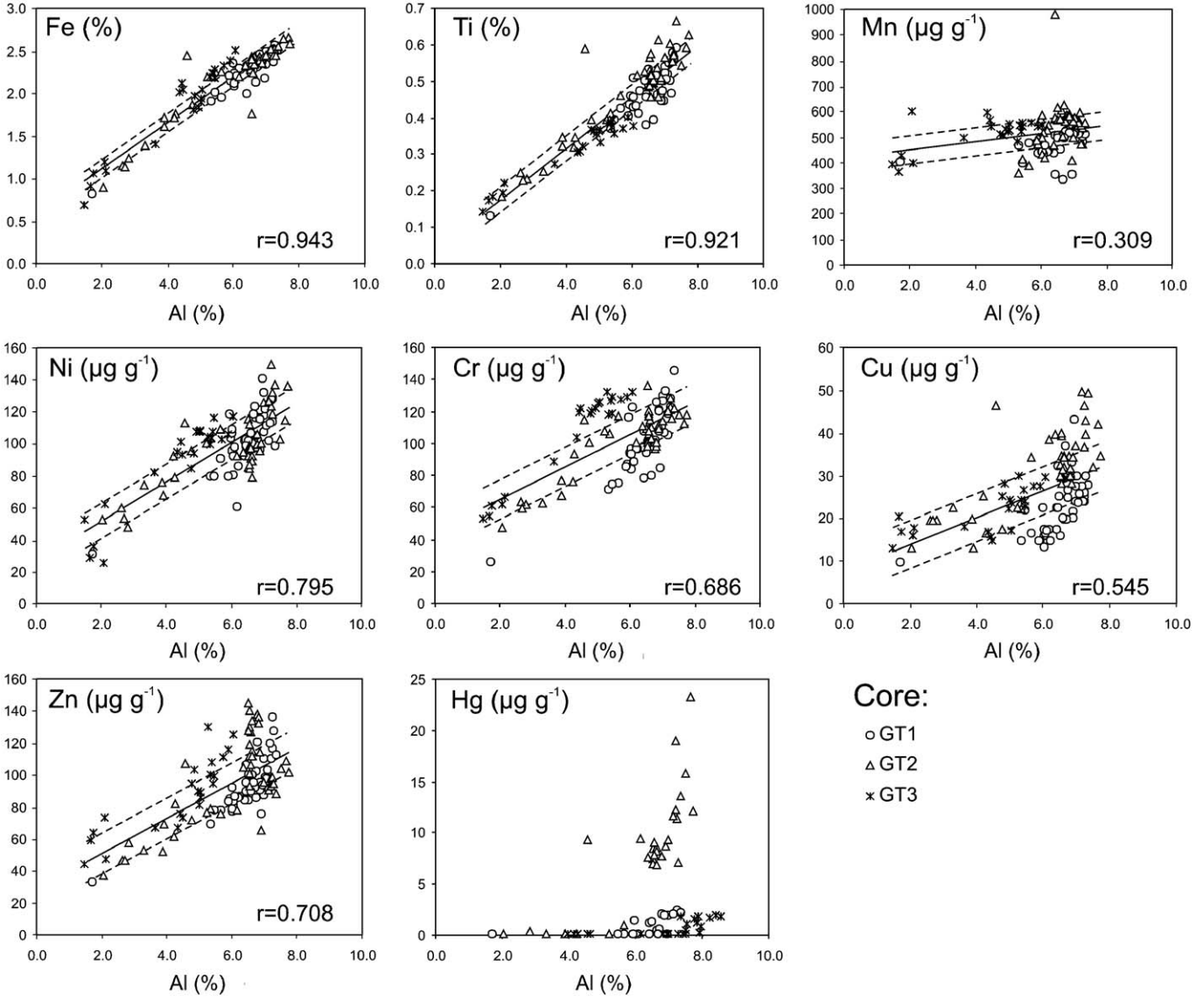

Fig. 6. Scatterplot between trace, major elements and Aluminium. The regression line and 95% confidence band are reported.

Table 3
Linear regression parameters between heavy metals and Aluminum for calculation of regional baselines (a=angular coefficient, b=y intercept, r=correlation coefficient, SEE=standard error estimate, N=number of samples)

Element	a	b	r	SEE	N
Fe (%)	0.275	0.531	0.985	0.031	93
Ti (%)	0.071	0.032	0.979	0.009	88
Mn (ppm)	22.169	383.623	0.700	15.038	86
Ni (ppm)	12.015	29.546	0.922	3.821	65
Cr (ppm)	10.799	38.277	0.911	3.660	72
Cu (ppm)	2.710	10.134	0.782	1.519	72
Zn (ppm)	11.225	23.713	0.904	3.660	75

All relations are significant at $P \leq 0.001$.

subsurficial layers: 8.5 cm for GT1 (EF=17.2), 49.5 cm for GT2 (EF=64.1) and 12.5 cm for GT3 (EF=9.5).

5.4. Accumulation rates and inventories of Hg

The long-term (ca. 500 yr) Hg mining activity at Idrija (Fig. 1) is well recorded in the sedimentary sequence of the Gulf of Trieste due to the accumulation of that part of metal lost during the excavation and smelting of more than 5×10^6 metric tons of ore, mostly cinnabar. The annual amount of cinnabar ore extracted and of Hg produced during the five centuries of mining activity was provided in detail by Mlakar (1974). As indicated in Fig. 8, Hg production can be dated back to about 1500, although the amount of ore excavated and metal produced increased dramatically between the end of the 18th century and the second half of the 20th century. The greatest annual amount of Hg produced occurred in 1913 (820 tons). If related to mining activity, it is realistic to consider that the contamination process due to metal dissipation into the environment followed a parallel development. Estimation of metal recovery from ore was about 60–70% until 1800 (Mlakar, 1974) during which time high amounts of cinnabar were released into the river in spite of the comparatively small volume of extracted ore. After 1800 the extraction recovery improved, and was up to more than 90% in the most recent times of major production. Biester et al. (2000) suggest that most of the Hg accumulated in fine-grained sediments from river terraces and in the Gulf could be due to the rising amount of mining residues and the intensive crushing of the ore that increased the amount of fine grained material and Hg concentrations in the core profiles.

As previously reported for core AA1 (Covelli et al., 2001), the cinnabar ore extraction and metal production records at Idrija (Fig. 8) correlate well with Hg concentration and Hg EF profiles in core GT2. In addition to the onset of the dramatic increase of Hg enrichment, which is common in all three cores, core GT2 records a very sharp peak in the top section corresponding to Hg enriched sediment deposition following maximum metal production at the Idrija mine (1913–1914). The Idrijca river and the surrounding region, as well as the whole Isonzo river basin, have a steep gradient and are characterized by high precipitation during the spring and autumn periods, which produces rapid run-off floods along with a high suspended sediment load due to erosion of river banks and surface soil. It can be reasonably assumed that the time lag between Hg loss during smelting activity in the Idrija region, remobilization and final deposition in the coastal area was relatively short. Thus a sharp peak in the Hg concentration in a core can be used as a chemostratigraphic marker and, since no other dating is available, the calendar ages can be assigned by assuming a constant accumulation rate from the marker sedimentary level to the present (Varekamp, 1991; Varekamp et al., 2003). This approach was successfully applied in the preliminary estimation of sedimentation rates in the mid-Gulf (core AA1), providing a value of 2.16 mm yr^{-1} on the basis of the Hg peak, whereas 1.84 mm yr^{-1} was obtained from ^{210}Pb determination for the same site (Covelli et al., 2001). If a similar procedure is applied for core GT2, an average sedimentation rate of 6 mm yr^{-1} is obtained. Since Hg profiles in core GT1 and GT3 do not show the evident sharp peak recognized in core GT2, the top sections of the two cores were dated with the onset of the Hg EF dramatic increase as a time marker (ca. 1800 AD). The estimated average sedimentation rates are 2.3 and 1.8 mm yr^{-1} for core GT1 and GT3, respectively. These results agree quite well with those based on ^{210}Pb analysis reported by Ogorelec et al. (1991) for the mid-Gulf area, ranging from about 1 to 2.5 mm yr^{-1}. Although mining activity started at the end of 15th century, sediment cores do not show evidence of the onset of Hg anthropogenic enrichment until the dramatic increase in the activity (ca. 1800 AD) because the perturbation of mining practices was probably not sufficient to be recorded in the sedimentary sequence.

Taking into account the rate at which sediment is accumulating at each site of core collection, the Hg

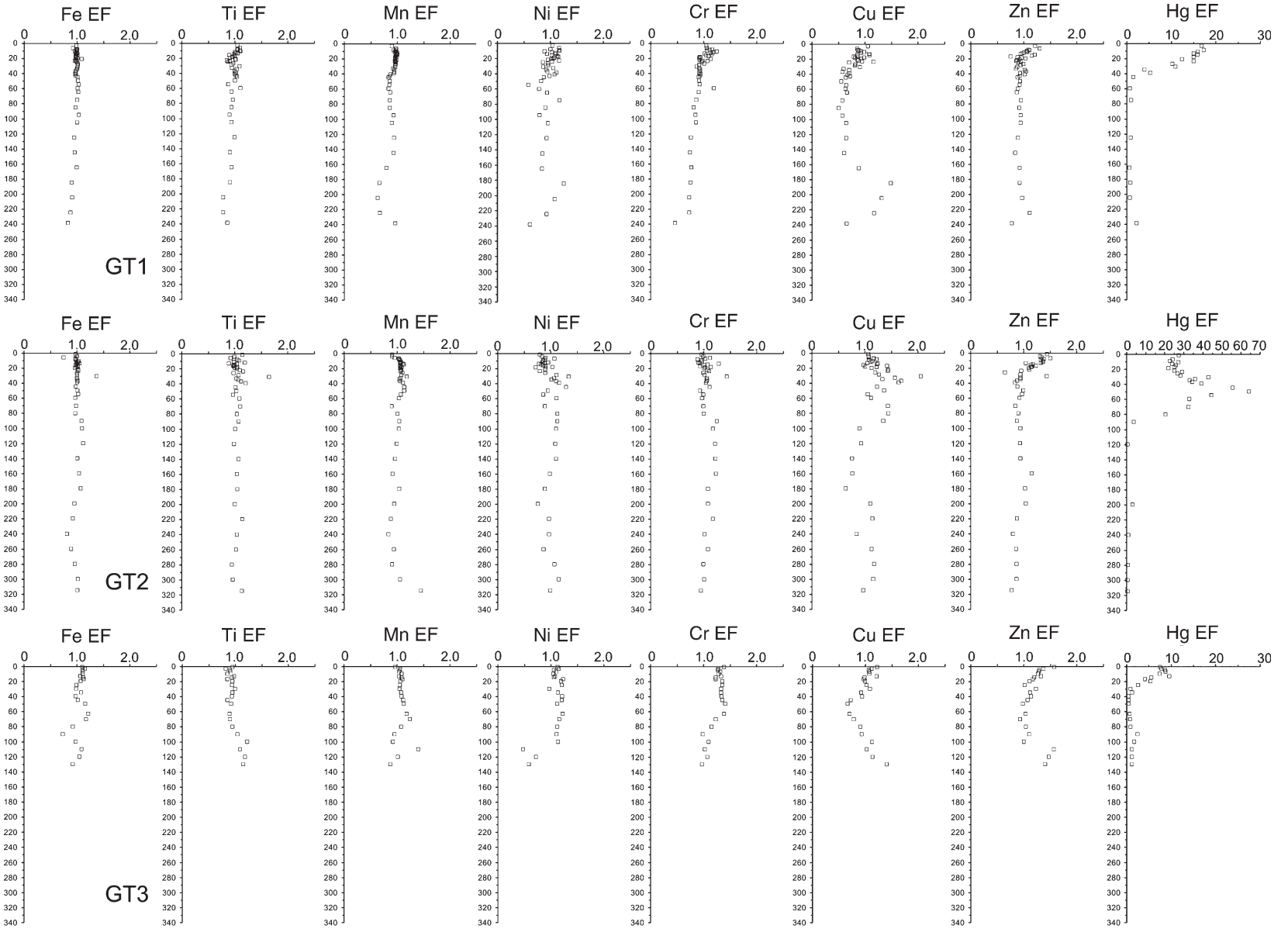

Fig. 7. Vertical enrichment profiles (EF) of trace metals in core sediments.

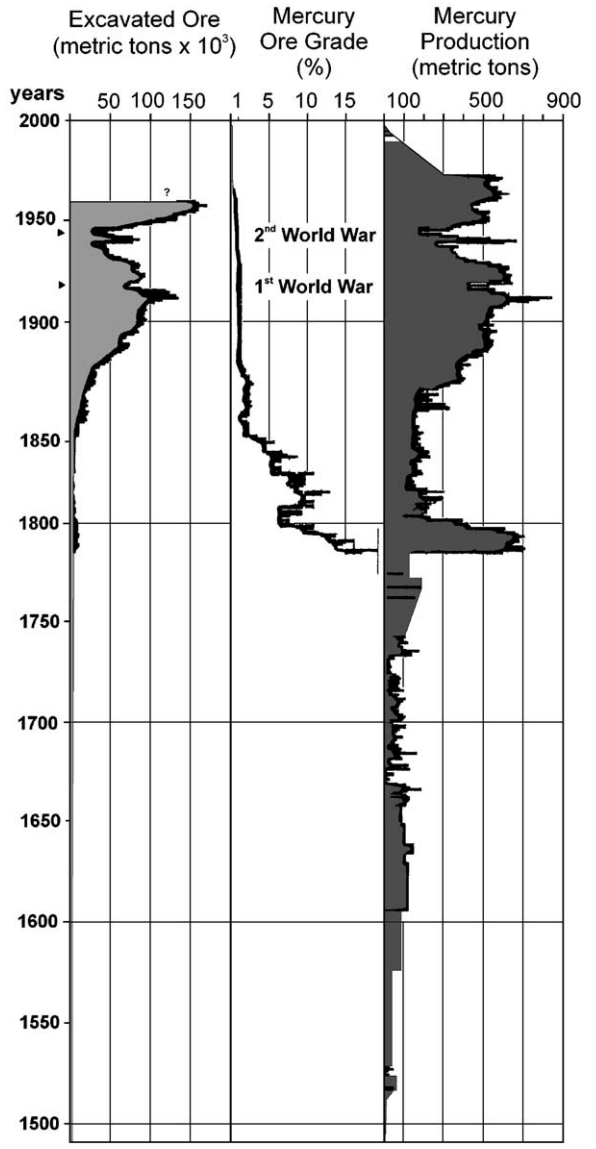

Fig. 8. Hg production and cinnabar ore extracted at Idrija (Slovenia) during 500 years of mining activity (adapted and redrawn from Mlakar, 1974).

accumulation rate (HgAR) in sediments is calculated from the following equation:

$$\text{HgAR (mg m}^{-2}\text{yr}^{-1}) = \omega(\text{Hg})s10^4$$

$$\text{with} \qquad \omega = (1-\varphi)v\rho$$

where ω is the mass sedimentation rate (g m^{-2} yr^{-1}), (Hg)s is Hg concentration (μg g^{-1}) in sediment, φ is porosity, v is sedimentation rate (mm yr^{-1}) and ρ is sediment density (g cm^{-3}). In spite of the mine closure (1996), the modern accumulation rate of Hg in the Gulf is very high and variable according to the distance from the Isonzo river mouth (Table 4). Whereas HgAR is estimated to be 1.77 mg m^{-2} yr^{-1} in the central sector of the Gulf, it reaches 31.49 mg m^{-2} yr^{-1} in front of the fluvial source (GT2). Intermediate HgAR of 3.75 and 4.23 mg m^{-2} yr^{-1}, respectively, are recorded in GT1 and AA1 (Covelli et al., 2001). The maximum rate of HgAR reaches up to four orders of magnitude (139.71 mg m^{-2} yr^{-1}) higher than the background accumulation rate in GT2 (Table 4). Temporal variations of Hg loading show a decrease to the present day in all three cores (Fig. 9). The pre-1800 HgAR appears to be from one to two orders of magnitude lower than the most recent flux.

Vertical profiles of Hg concentration in core sediments collected off the river Po delta also show enriched surficial layers, ranging between 50 and 230 ng g^{-1} attributed to anthropogenic sources (Fabbri et al., 2001). The river Po is recognised as the main sedimentary input to the northern Adriatic Sea with an apparent sedimentation rate in the nearshore prodelta zone of the order of 2–4 cm yr^{-1} (Boldrin et al., 1988). However, the Hg accumulation rate off the river Po delta is only 0.75 mg m^{-2} yr^{-1} (Coquery et al., 1996) which is equivalent to the pre-mining accumulation rate estimated in front of the Isonzo river mouth (GT2). Sediments of the Gulf of Trieste are undoubtedly the final sink for most of the anthropogenic Hg lost during the long-term mining activity in Idrija.

The cumulative Hg inventory quantifies the total amount of the metal loaded to the sediments over time (Kolak et al., 1998). If the natural input of Hg is removed by subtracting the background concentration from total concentration, the inventory represents the anthropogenic loading of Hg calculated as follows:

$$\text{Hg Inv (mg m}^{-2}) = \sum[(\text{Hg}^*)s(1-\varphi)\rho d]$$

where (Hg*)s is the background corrected concentration in the sediment and d is the thickness of sediment between analysed core levels. The cumulative Hg* inventory is the total mass of Hg due to mining residues that was deposited on a 1 m^2 surface area over the maximum period of Hg production and contamination (1800–1996). The results show a very large difference between Hg* inventory in core GT2 and the remaining three cores, thus indicating that most of the metal accumulates in the shallow waters in the vicinity of the Isonzo River mouth following the rapid decrease of the fluvial current (Table 4). Previous studies demonstrated that in surface sediments detrital cinnabar is the prevalent form of Hg present in sandy-silty sediments

Table 4
Hg background values (μg g^{-1}), surface, peak, average (post 1800) and pre-mining activity Hg accumulation rates, cumulative inventories of Hg for each core in the period 1800–1996 and estimated average sedimentation rates

	Hg background (μg g^{-1})	Hg total accumulation rate post 1800 (mg m^{-2} yr^{-1})			Hg pre-mining accumulation rate (mg m^{-2} yr^{-1})	Hg[a] inventory (1800–1996) (mg m^{-2})	Estimated avg. sed. rate (mm yr^{-1})
		Surface	Peak	Average			
GT1	0.083	3.75	4.22	3.02	0.18	509	2.3
GT2	0.149	31.49	139.71	52.84	0.76	8556	6.0 (3.5[b])
GT3	0.101	1.77	2.79	1.70	0.22	249	1.8
AA1	0.168	4.23	8.81	4.94	0.40	734	2.2 (2.1[b])

[a] Background corrected concentration.
[b] Calculated between 1800 and 1913.

whereas the metal would be associated with finer particles (silty-clay fraction) in the form of Hg^{2+}, Hg^{+} and Hg^{0} in offshore sediments (Biester et al., 2000; Covelli et al., 2001).

Based on these Hg* inventories, a rough estimation of the total amount of Hg buried in the marine sediments of the Gulf since the rapid increase of Hg ore extraction (ca. 1800) can be attempted. Although a large number of core profiles would be necessary to better define the spatial variability of Hg in the sedimentary sequence, and assuming a symmetrical dispersion of the riverborne material for simple calculation, the result amounts to about 900 tonnes. This quantity is only 1/40 of the 23% of the total mercury extracted (144,000 tonnes), which is estimated to have been dispersed into the environment (Gosar et al., 1996). In fact, because of emissions from the roasting plant chimney and ventilation shaft, elemental and particulate Hg have been released into the air (Gosar et al., 1996) and they have subsequently enriched soil in the Idrija area through atmospheric fallout (Biester et al., 1998). In addition, during the plant's operation the roasted cinnabar residues were dumped along the banks of the Idrijca river and subsequently swept away by water flooding towards the Isonzo River and downstream into the Gulf of Trieste. This apparently underestimated result could be due to the combined responses of the storage of large volumes of Hg-enriched soils and overbank sediments along the Isonzo river drainage basin (Horvat et al., 2002) and also in the bottom sediments of the adjacent Grado and Marano lagoons (Piani et al., 2005). This observation is also supported by the high metal concentrations (up to 14 μg g^{-1}) and thickness of contaminated sediments (20–30 cm) found in the eastern sector of the lagoons (Brambati, 1997). Through the easternmost tidal inlet, riverborne Hg bound to fine suspended particles flows into the lagoon carried by tidal currents and only gradually accumulating at the bottom after several tidal cycles.

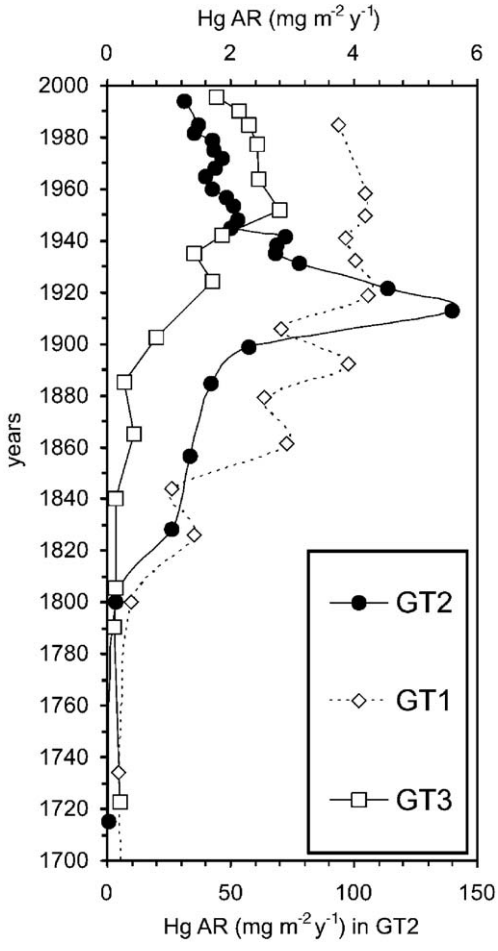

Fig. 9. Estimated accumulation rate of Hg in core sediments.

6. Conclusions

The stratigraphic record of core sediments from the Gulf of Trieste, which were analyzed for changes

produced in sedimentological and geochemical features during the Holocene, provided undoubted remarks not only from the paleoenvironmental point of view but also regarding the impact assessment of anthropogenic activities using trace metals as indicators. The following results are highlighted:

(1) ^{14}C datings on bulk sedimentary OC as well as on shell samples in the basal part of the three cores ranged between 8270±50 and 9610±40 yr BP. In addition to the highly negative $\delta^{13}C_{org}$ values and micropaleontological and lithological evidence, these results show that lacustrine-swamp conditions were still present in the northernmost sector of the Adriatic Sea at that time, as documented in previous regional studies. Sea level-rise and environmental change to typical marine depositional conditions were rapid and, presumably, not contrasted by high sedimentation rates at local scale, at least, at the beginning of the marine transgression.

(2) Cluster and PCA analyses applied to the whole analytical dataset helped to distinguish homogeneous stratigraphic units. Each unit may be interpreted in terms of either paleoenvironmental change, or cultural perturbation. The maximum horizon depth "perturbated" by human activities corresponds to the uppermost stratigraphic unit, easily discernible by the mutual relationships between natural (Fe, Al, Ti, Ni, Cr) and anthropogenic (Hg, Cu and Zn) elements.

(3) Metal background values in the cores can be used as references for the assessment of anthropogenic enrichment factors of coastal sediments in the area, through the application of simple metal-Al linear relationships. Whereas moderate contamination of Cu and Zn was detected at the core top, significant Hg enrichment, far above the average estimated background value for the Gulf (0.13 μg g^{-1}), occurred upcore, especially in front of the Isonzo River mouth (GT2), as a consequence of the long-term mining activity at Idrija (Slovenia).

(4) The historical development of Hg contamination is well recorded in core sediments and it varies according to Hg data production since the beginning of the 1800s when extraction activity began to grow exponentially. Estimated sedimentation rates for the last 100 yr appear to be reasonable using Hg as chemostratigraphic marker. Recent Hg accumulation rates in the Gulf of Trieste are from one to two orders of magnitude higher than the Po river's, the main freshwater supply of sediments in the Adriatic Sea. The Isonzo river is undoubtedly the main source of the metal in this marine basin.

(5) The cumulative Hg inventory allowed us to estimate roughly the amount of metal buried in the sediments of the Gulf, which can be considered as an important "reservoir" for the metal. However, the results seem to indicate that only a small part of Hg extracted and lost in the environment is stored within marine sediments, suggesting that large amounts of Hg are still present in the drainage basin of the Isonzo River. As a consequence, although Hg fluxes into the Gulf have decreased in recent times, natural attenuation as a passive decontamination approach for sediment remediation seems to be the only long-term solution since Hg inputs will be supplied by river waters during flood events.

Acknowledgements

The authors are grateful to Loris Sartore and Giuseppe Buzzi for their valuable work on laboratory analyses. John Ridgway and two anonymous reviewers are warmly acknowledged for their critical review of the manuscript and their useful suggestions. Many thanks are due to the crew of the R/V OGS Explora for field support during core sampling. This work was partially supported by grants from the bilateral scientific-technologic co-operation Italy-Slovenia (Ministry of Foreign Affairs).

References

Adami, G., Barbieri, P., Campisi, B., Predonzani, S., Reisenhofer, E., 1996. Anthropogenic heavy metal distribution in sediments from an area exposed to industrial pollution (harbour of Trieste, Northern Adriatic Sea). Boll. Soc. Adriat. Sci. 77, 5–18.

Adami, G., Barbieri, P., Piselli, S., Predonzani, S., Reisenhofer, E., 1998. New data on organic pollutants in surface sediments in the harbour of Trieste. Ann. Chim. 88, 745–754.

Albani, A.D., Serandrei Barbero, R., 1990. I foraminiferi della laguna e del Golfo di Venezia. Mem. Sci. Geol., Univ. Padova 42, 271–341.

Amorosi, A., Colalongo, M.L., Pasini, G., Preti, D., 1999. Sedimentary response to Late Quaternary sea-level changes in the Romagna coastal plain (northern Italy). Sedimentology 46, 99–121.

Berner, R.A., 1980. Early Diagenesis—A Theoretical Approach. Princeton University Press, Princeton, New York, p. 241.

Biester, H., Hess, A., Müller, G., 1998. Mercury phases in soils and sediments in the Idrija mining area. In: Miklavcic, V. (Ed.), Idrija as a Natural and Anthropogenic Laboratory: Mercury as a Major

Pollutant, Book of Proceedings, Meeting of Researchers, May 1996. Idrija Mercury Mine, Idrija, pp. 17–21.
Biester, H., Gosar, M., Covelli, S., 2000. Mercury speciation in sediments affected by dumped mining residues in the drainage area of the Idrija mercury mine. Environ. Sci. Technol. 34, 3330–3336.
Boldrin, A., Bortoluzzi, G., Frascari, F., Guerzoni, S., Rabitti, S., 1988. Recent deposits and suspended sediments off the Po della Pila (Po river, main mouth), Italy. Mar. Geol. 79, 159–170.
Bortolami, G., Fontes, J.C., Markgraf, V., Barker, E.D., 1977. Land, sea and climate in the northern Adriatic region during late Pleistocene and Holocene. Paleogeogr. Paleoclimatol. Paleoecol. 21, 139–156.
Brambati, A., 1970. Provenienza, trasporto e accumulo dei sedimenti recenti nelle lagune di Marano e di Grado e nei litorali tra i fiumi Isonzo e Tagliamento. Mem. Soc. Geol. Ital. 9, 281–329.
Brambati, A., 1997. Metalli pesanti nelle lagune di Marano e Grado. Piano di studi finalizzato all'accertamento di sostanze persistenti nelle Lagune di Marano e Grado ed al loro risanamento. (RFVG) Direzione Regionale dell'Ambiente, Servizio dell'Idraulica, Trieste. 174 pp.
Brambati, A., Venzo, G.A., 1967. Recent sedimentation in the Northern Adriatic Sea between Venice and Trieste. Studi Trentini Sci. Nat. 44, 202–274.
Brambati, A., Ciabatti, M., Fanzutti, G.P., Marabini, F., Marocco, R., 1983. A new sedimentological textural map of the Northern and Central Adriatic Sea. Boll. Oceanol. Teor. Appl. 1, 267–271.
Colizza, E., Fontolan, G., Brambati, A., 1996. Impact of a coastal disposal site for inert wastes on the physical marine environment, Barcola-Bovedo, Trieste, Italy. Environ. Geol. 27, 270–285.
Coquery, M., Cossa, D., Gobeil, C., Azemard, S., Sanjuan, J., Magand, O., Horvat, M., 1996. The significance of mercury and methylmercury profiles in coastal sediments. In: Ebinghaus, R., Petersen, G., von Tümpling, U. (Eds.), Book of Abstracts IV International Conference "Mercury as a Global Pollutant", 4–8 August 1996, Hamburg, Germany, p. 501.
Correggiari, A., Field, M.E., Trincardi, F., 1996a. Late Quaternary transgressive large dunes on the sediment-starved Adriatic shelf. In: De Batist, M., Jacobs, J. (Eds.), Geology of Siliciclastic Shelf Seas. Geological Society Special Publications, vol. 117, pp. 155–169.
Correggiari, A., Roveri, M., Trincardi, F., 1996b. Late Pleistocene and Holocene evolution of the north Adriatic Sea. Il Quaternario. Ital. J. Quat. Sci. 9, 697–704.
Covelli, S., Fontolan, G., 1997. Application of a normalization procedure in determining regional geochemical baselines: Gulf of Trieste, Italy. Environ. Geol. 30, 34–45.
Covelli, S., Horvat, M., Faganeli, J., Brambati, A., 1999. Pore water distribution and benthic fluxes measurements of mercury and methylmercury in the Gulf of Trieste (Northern Adriatic Sea). Estuar. Coast. Shelf Sci. 48, 415–428.
Covelli, S., Faganeli, J., Horvat, M., Brambati, A., 2001. Mercury contamination of coastal sediments as the result of long-term cinnabar mining activity (Gulf of Trieste, northern Adriatic Sea). Appl. Geochem. 16, 541–558.
Fabbri, D., Gabbianelli, G., Locatelli, C., Lubrano, D., Trombini, C., Vassura, I., 2001. Distribution of mercury and other heavy metals in core sediments of the northern Adriatic Sea. Water Air Soil Pollut. 129, 143–153.
Faganeli, J., Ogorelec, B., Misic, M., Dolenec, T., Pezdic, J., 1987. Organic geochemistry of two 40-m sediment cores from the Gulf of Trieste (Northern Adriatic). Estuar. Coast. Shelf Sci. 25, 157–167.
Faganeli, J., Planinic, R., Pezdic, J., Smodis, B., Stegnar, P., Ogorelec, B., 1991. Marine geology of the Gulf of Trieste (northern Adriatic): geochemical aspects. Mar. Geol. 99, 93–108.
Fairbanks, R.G., 1989. A 17,000-year glacio-eustatic sea level record: Influence of glacial melting rates on the Younger Dryas event and deep-ocean circulation. Nature 342, 637–642.
Fairbanks, R.G., 1990. The age and origin of the "Younger Dryas climate event" in Greenland ice cores. Paleoceanography 5, 937–948.
Gosar, M., Pirc, S., Sajn, R., Bidovec, M., Mashyanov, N.R., Sholupov, S.E., 1996. Mercury in the air: pollution in Idrja, Slovenia. In: Ebinghaus, R., Petersen, G., von Tümpling, U. (Eds.), Book of Abstracts IV International Conference "Mercury as a Global Pollutant", 4–8 August 1996, Hamburg, Germany, p. 468.
Gosar, M., Pirc, S., Bidovec, M., 1997. Mercury in the Idrijca River sediments as a reflection of mining and smelting activities of the Idrija mercury mine. J. Geochem. Explor. 58, 125–131.
Hedges, J.I., Stern, J.H., 1984. Carbon and nitrogen determinations in carbonate-containing solids. Limnol. Oceanogr. 29, 657–663.
Hornberger, M.I., Luoma, S.N., Van Geen, A., Fuller, C., Anima, R., 1999. Historical trends of metals in the sediments of San Francisco Bay, California. Mar. Chem. 64, 39–55.
Horvat, M., Jereb, V., Fajon, V., Logar, M., Kotnik, J., Faganeli, J., Hines, M.E., Bonzongo, J.-C., 2002. Mercury distribution in water, sediment, and soil in the Idrijca and Soca River systems. Geochem., Explor. Environ. Anal. 2, 287–296.
Huh, C.-A., 1996. Fluxes and budgets of anthropogenic metals in the Santa Monica and San Pedro Basins off Los Angeles: review and reassessment. Sci. Total Environ. 179, 47–60.
INTERREG II, 2001. Progetto di monitoraggio dell'Alto-Adriatico–Relazione Conclusiva, Luglio 1998–Giugno 2001. Direzione Regionale dell'Ambiente, Laboratorio di Biologia Marina, Trieste, Italia, p. 112.
Kolak, J.J., Long, D.T., Beals, T.M., 1998. Anthropogenic inventories and historical and present acuumulation rates of copper in Great Lakes sediments. Appl. Geochem. 13, 59–75.
Lapp, B., Balzer, W., 1993. Early diagenesis of trace metals used as an indicator of past productivity changes in coastal sediments. Geochim. Cosmochim. Acta 57, 4639–4652.
Loring, D.H., 1990. Lithium—a new approach for the granulometric normalization of trace metal data. Mar. Chem. 26, 155–168.
Loring, D.H., 1991. Normalization of heavy-metal data from estuarine and coastal sediments. ICES J. Mar. Sci. 48, 101–115.
Loring, D.H., Rantala, R.T.T., 1992. Manual for the geochemical analyses of marine sediments and suspended particulate matter. Earth-Sci. Rev. 32, 235–283.
Marocco, R., 1991. Evoluzione tardopleistocenica-olocenica del delta del F. Tagliamento e delle Lagune di Marano e Grado (Golfo di Trieste). Il Quat. 4, 223–232.
Meyers, P.A., 1997. Organic geochemical proxies of paleoceno-graphic, paleolimnologic and paleoclimatic processes. Org. Geochem. 27, 213–250.
Mlakar, L., 1974. An outline of production of the Idrija mercury mine through the centuries. Idrij. Razgl. 3–4, 1–115.
Mosetti, F., 1966. Morfologia dell'Adriatico settentrionale. Boll. Geofis. Teor. Appl. 8, 138–150.
Mosetti, F., 1983. Sintesi sull'idrologia del Friuli-Venezia Giulia. Quaderni dell'Ente Tutela Pesca, vol. 6, pp. 1–295.
Munsell Soil Color Charts, 1975. Macbeth Division of Kollmorgen Corporration, Baltimore, Maryland.

Ogorelec, B., Misic, M., Sercelj, A., Cimerman, F., Faganeli, J., Stegnar, P., 1981. The sediment of the saltmarsh of Secovlje. Geologija 24, 179–216.

Ogorelec, B., Misic, M., Faganeli, J., Sercelj, A., Cimerman, F., Dolenec, T., Pezdic, J., 1984. Quaternary sediment of the borehole V-3 in the Bay of Koper. Slov. Morje Zaledje, Ljubljana 6/7, 165–186.

Ogorelec, B., Misic, M., Faganeli, J., Stegnar, P., Vriser, B., Vukovic, A., 1987. The recent sediment of the Bay of Koper (Northern Adriatic). Geologija 30, 87–121.

Ogorelec, B., Misic, M., Faganeli, J., 1991. Marine geology of the Gulf of Trieste (northern Adriatic): sedimentological aspects. Mar. Geol. 99, 79–92.

Ogorelec, B., Faganeli, J., Misic, M., Cermelj, B., 1997. Reconstruction of paleoenvironment in the Bay of Koper (Gulf of Trieste, northern Adriatic). Annales 11, 187–200.

Ogrinc, N., Fontolan, G., Faganeli, J., Covelli, S., 2005. Carbon and nitrogen isotope compositions of organic matter in coastal marine sediments (the Gulf of Trieste, N Adriatic Sea): indicators of sources and preservation. Mar. Chem. 95, 163–181.

Olivotti, R., Faganeli, J., Malej, A., 1986. Impact of 'organic' pollutants on coastal waters, Gulf of Trieste. Water Sci. Technol. 18, 57–68.

Piani, R., Covelli, S., Biester, H., 2005. Mercury contamination in Marano Lagoon (Northern Adriatic Sea, Italy): source identification by analyses of Hg phases. Appl. Geochem. 20, 1546–1559.

Preti, M., 1999. The Holocene transgression and the land–sea interaction south of the Po delta. G. Geol. 61, 143–159.

RAFVG, 1986. Caratteristiche chimico-fisiche e biologiche dei corpi idrici superficiali e profondi della regione (Allegato 5). Regione Friuli-Venezia Giulia, Direzione Regionale dell'Ambiente, Servizio per l'utilizzazione delle acque.

Rossi, S., Mosetti, F., Cescon, B., 1968. Morfologia e natura del fondo nel Golfo di Trieste (Adriatico settentrionale fra Punta Tagliamento e Punta Salvore). Boll. Soc. Adriat. Sci. 56, 187–206.

Schropp, S.J., Graham Lewis, F., Windom, H.L., Ryan, J.D., Calder, F.D., Burney, L.C., 1990. Interpretation of metal concentrations in estuarine sediments of Florida using Aluminum as a reference element. Estuaries 13, 227–235.

Serandrei Barbero, R., Albani, A.D., Favero, V.M., 1989. Distribuzione dei foraminiferi recenti nella Laguna di Venezia. Boll. Soc. Geol. Ital. 108, 279–288.

Skowronek, F., Sagemann, J., Stenzel, F., Schulz, H.D., 1994. Evolution of heavy-metal profiles in River Weser Estuary sediments, Germany. Environ. Geol. 24, 223–232.

Stefanini, S., 1976. Composizione delle acque fluviali del Friuli-Venezia Giulia durante la fase di magra e di piena dei corsi d'acqua. CNR Quaderni dell'Istituto di Ricerca sulle Acque, 28, pp. 391–447.

Trincardi, F., Correggiari, A., Roveri, M., 1994. Late Quaternary transgressive erosion and deposition in a modern epicontinental shelf: the Adriatic semienclosed basin. Geo Mar. Lett. 14, 41–51.

Varekamp, J.C., 1991. Trace element geochemistry and pollution history of mudflat and marsh sediments from the Connecticut coastline. J. Coast. Res. 11, 105–123.

Varekamp, J.C., Kreulen, B., Buchholtz Ten Brink, M.R., Mecray, E. L., 2003. Mercury contamination chronologies from Connecticut wetlands and Long Island Sound sediments. Environ. Geol. 43, 268–282.